Author Manuscript

Author Manuscript

Author Manuscript

Author Manuscript

HHS Public Access

Author manuscript

J Microbiol Methods. Author manuscript; available in PMC 2017 November 15.

Published in final edited form as:

J Microbiol Methods. 2012 August ; 90(2): 119–133. doi:10.1016/j.mimet.2012.04.007.

A gel-free proteomic-based method for the characterization of *Bordetella pertussis* clinical isolates

Yulanda M. Williamson[a], **Hercules Moura**[a], **Kaneatra Simmons**[b], **Jennifer Whitmon**[b], **Nikkol Melnick**[b], **Jon Rees**[a], **Adrian Woolfitt**[a], **David M. Schieltz**[a], **Maria L. Tondella**[b], **Edwin Ades**[b], **Jacquelyn Sampson**[b], **George Carlone**[b], and **John R. Barr**[a,*]

[a]Division of Laboratory Sciences, National Center for Environmental Health, Centers for Disease Control and Prevention, Chamblee, Georgia 30341, USA

[b]Division of Bacterial Diseases, National Center for Immunizations and Respiratory Diseases, Centers for Disease Control and Prevention, Atlanta, Georgia 30333, USA

Abstract

Bordetella pertussis (*Bp*) is the etiologic agent of pertussis or whooping cough, a highly contagious respiratory disease occurring primarily in infants and young children. Although vaccine preventable, pertussis cases have increased over the years leading researchers to re-evaluate vaccine control strategies. Since bacterial outer membrane proteins, comprising the surfaceome, often play roles in pathogenesis and antibody-mediated immunity, three recent *Bp* circulating isolates were examined using proteomics to identify any potential changes in surface protein expression. Fractions enriched for outer membrane proteins were digested with trypsin and the peptides analyzed by nano liquid chromatography-electrospray ionization-mass spectrometry (nLC-ESI-MS), followed by database analysis to elucidate the surfaceomes of our three *Bp* isolates. Furthermore, a less labor intensive non-gel based antibody affinity capture technology in conjunction with MS was employed to assess each *Bp* strains' immunogenic outer membrane proteins. This novel technique is generally applicable allowing for the identification of immunogenic surface expressed proteins on pertussis and other pathogenic bacteria.

Keywords

Pertussis; Proteomics; Membrane; Gel-free; LC-MS/MS; Antibody-affinity

1. Introduction

Bordetella pertussis (*Bp*) is the etiologic agent of pertussis or whooping cough, a highly contagious respiratory disease occurring primarily in infants and young children (Bordet and Gengou, 1906; Singh and Lingappan, 2006). Current vaccines used in the United States are acellular. They consist of three to five *Bp* proteins (Locht, 2008; Taylor and Fahm, 1999), including filamentous hemagglutinin adhesin (FHA), pertactin (Prn), pertussis toxin (Ptx),

Open access under CC BY-NC-ND license.

*Corresponding author at: 4770 Buford Highway, MS-F50, Chamblee, Georgia 30341, USA. Tel.: +1 770 488 7848 (Office); fax: +1 770 488 0509. jbarr@cdc.gov (J.R. Barr).

Author Manuscript Author Manuscript Author Manuscript Author Manuscript

and fimbrae 2 and 3. These latter proteins are purified from *Bp* strains isolated from the 1940s and 1950s. Many countries throughout the world, however, continue to use whole-cell vaccines. Although pertussis is a vaccine-preventable disease, the World Health Organization (WHO) estimates that 30–50 million cases per year occur worldwide, with approximately 300,000 deaths (http://www.cdc.gov/). In fact, pertussis cases have increased over the years, leading researchers to reevaluate vaccine control strategies. This resurgence in pertussis cases has occurred globally (King et al., 2001; Das, 2002) and has occurred in populations or areas previously immunoprotected by vaccination. Although the cause for the observed increased disease incidence is not fully understood, possible contributing factors are better diagnostics and surveillance, waning vaccine-induced immunity, suboptimal vaccine formulation, and variation between circulating isolates and vaccine strains (He and Mertsola, 2008; Matoo and Cherry, 2005; Bart et al., 2010) which are all currently under investigation.

With the sequencing of many microbial pathogen genomes complete (Parkhill et al., 2003) or underway, many researchers have relied on functional genomics to translate the genetic “blueprint” of an organism and to understand biological processes. But with constantly advancing methods and technologies, the use of proteomic-based strategies has emerged as an option to study cellular function. In general, proteomics revolutionized in the mid 1970s (O'Farrell, 1975; Wilkins et al., 2007) is the analysis of an organism's proteome or, in essence, its complete array of expressed genes or proteins.

Traditional proteomic approaches, such as one- (1D) or two-dimensional (2D) gel electrophoresis (GE), are common technologies to visualize and separate proteins based on molecular weight and/or isolectric point (pI). 1D and 2D-GE, albeit fruitful, can be labor intensive and not without technical challenges. For instance, 1D-GE cannot sufficiently resolve very large proteins or complexes that generally are membrane-affiliated and hydrophobic in nature. Also, small proteins often expressed in low abundance may escape visual detection dependent upon the rate of gel migration (Kustos et al., 2007). However, to overcome these limitations subcellular compartments, such as outer membrane proteins (OMPs) or surfaceomes can be isolated by physical or chemical means, and further enriched using sodium carbonate (Thein et al., 2010) followed by differential centrifugation. Fractionation reduces sample complexity and promotes further examination by GE or mass spectrometry (MS). Nano liquid chromatography-electrospray ionization tandem MS (nLC-ESI MS/MS) is a powerful and sensitive analytical tool used to further elucidate and characterize proteins in complex mixtures (Dworzanski and Snyder, 2005; Han et al., 2008). Proteins can be proteolytically cleaved by enzymes such as trypsin, generating peptides that are first separated by differential retention on the LC column then ionized and separated based on their mass-to-charge ratio (m/z). The proteins from which they originate are identified based on the comparison between MS/MS fragmentation patterns and protein databases (Chen and Prama, 2008).

Over the years, gel-based strategies in parallel with MS have been used with great success in the characterization of bacterial surfaceomes (surface membrane fraction). For example, Somner et al. (2010) performed a comparative surfaceome analysis of pathogenic enterotoxigenic *Escherichia coli* (ETEC) and commensal strains using gel and MS-based

Author Manuscript Author Manuscript Author Manuscript Author Manuscript

proteomic approaches. In addition, nLC-ESI MS/MS analysis was used to profile the surfaceome of four genetically distinct *Staphylococcus aureus* strains (Dreisbach et al., 2010). Thein et al. (2010) evaluated the efficiency of multiple surfaceome isolations using nLC-ESI MS/MS, GE, and immunoblotting methodologies for OMP identification of various gram negative bacteria, including *Pseudomonas aeruginosa*. And Jabbour et al. (2010) performed a high-throughput proteomics study using nLC-ESI MS/MS to identify cellular proteins from pathogenic *E. coli* 0157:H7 and *Yersinia pestis*. Lastly, Bottero et al. (2007) described a procedure for the enrichment of *Bp* outer membrane proteins (OMPs) followed by protein identification using GE-associated mass spectrometric technologies and database search analysis as the basis for novel pertussis vaccine development.

Bp, a gram-negative organism, contains outer and cytoplasmic (or inner) membranes separated by a periplasmic space. Proteins embedded within the membrane and surface-exposed are of biological importance. These bacterial proteins act as front-line barriers to the hosts' antibody-mediated cellular environment. They contain possible virulence factors, and they play a role in the attachment to host cells as well as in the transport of nutrients into the bacteria needed for growth and survival (Poolman et al., 1990; van den Berg et al., 1999; Kustos et al., 2007; Lee et al., 2008). Thus, further examination of this subproteome (in particular for clinical pathogens) by GE or advanced technologies such as MS, would be fruitful for the development of novel diagnostics, strain comparison, or potentially for improved vaccine development.

In this study, a comparative qualitative proteomic assessment of three clinical *Bp* strains isolated in the United States and the well-typed acellular and whole-cell vaccine strain Tohama I was investigated. Since changes in OMP expression might affect several bacterial functions such as adherence and pathogenesis with possible implications on host cellular immunity (Kustos et al., 2007; Jabbour et al., 2010), we examined the surfaceome and immunoproteome (i.e., antigenic proteins that invoke an immune response). Protein profiles were generated using a multi-combinatorial approach of 1D-GE and/or direct nLC-ESI MS/MS tryptic peptide detection and OMP identification via database search analysis. Additionally, immunoblot-associated MS analysis and a novel approach using antibody affinity magnetic-bead-capture coupled to MS were used to identify *Bp* immunoreactive proteins. This antibody affinity, magnetic-bead-capture technique proved to be a labor-saving strategy that assisted in the quick assessment of *Bp* protein immunoreactivity. This strategy shows great promise as an expeditious approach – applicable to a broad spectrum of organisms – to identify surface-expressed antigens which, once detected and identified, could be used for strain comparisons and for improved diagnostics.

2. Materials and methods

Fig. 1 is a flow diagram schematically summating the core methodologies used in this study.

2.1. Reagents

All reagents and media not vendor-specified were prepared at the Centers for Disease Control and Prevention (CDC) Core Facility. In addition, chemicals used in experimentation

Author Manuscript Author Manuscript Author Manuscript Author Manuscript

were obtained from either Sigma-Aldrich Chemical Company (St. Louis, MO, USA) or Fisher Scientific (Pittsburg, PA, USA) as noted.

2.2. Bacterial strains

Four *Bp* strains, Tohama I (T) and three clinical isolates designated by CDC as C056 (C), D946 (D) and F656 (F) were used in the proteomic comparison (Table 1). T, first isolated in Japan in 1954, is a well-characterized and completely sequenced *Bp* strain that has been used as the basis of vaccines in many countries for several years (Advani et al., 2004). By pulse-field gel electrophoresis (PFGE) analysis, it is characterized as type II and possesses the pertactin 1 (*prnA1*) and pertussis toxin (*ptxS1B*) genotype typical of prevaccine-era isolates (Advani et al., 2004; van Loo et al., 2002; Litt et al., 2009). Strain C was isolated in Minnesota in 1998, has a PFGE CDC type 10 (Hardwick et al., 2002), and a *prnA2, ptxS1A* genotype common among currently circulating isolates (Litt et al., 2009). The D strain, a clinical isolate identified in Georgia in 2002, has a PFGE CDC 21, *prnA1* and *ptxS1A* genotype. It has shown resistance to the antibiotic erythromycin. Lastly, the F strain (PFGE CDC 206, *prnA2, ptxS1A*) was isolated from a clinical case in 2007 in the Virgin Islands.

2.3. Bacterial cell culture

T, C, D, and F were plated on Bordet-Gengou agar and incubated at 35 °C with 5% CO_2 for 4 days (Hulbert and Cotter, 2009). The bacteria were subsequently subcultured into Modified Stainer-Schulte (MSS) media at 35 °C, with aeration at 200 rpm in a Beckman-Coulter shaker (Beckman-Coulter, Brea, CA, USA) until an optical 1.0 density was reached. The bacterial strains were then pelleted from MSS by centrifugation at 8000×*g* for 30 min (min) at 4 °C. The pellets were washed two times in distilled water (dH_2O) and stored at −70 °C for further use.

2.4. Enriched membrane fraction collection

Enriched membrane fractions (EMFs) were collected as previously described (Molloy, 2008) with the following modifications. Briefly, cell pellets of *Bp* isolates were allowed to thaw gently on ice. The pellets were French-pressed at 16,000 psi in 5 ml of a 50-mM Tris–HCl (pH 8.0) buffer containing a protease inhibitor cocktail added at the manufacturer's recommendation (GE Healthcare, Piscataway, NJ, USA), and 25U of benzonase to rupture bacterial cells. The lysates were centrifuged (8000×*g*, 20 min, 4 °C) to remove unbroken cells, and the supernatant containing the total extracted proteome was retained. 50 ml of ice-cold sodium carbonate (pH 11.0) was added to 5 ml of each bacterial supernatant. The mixture was stirred gently at 4 °C for 2 h. The sodium carbonate infused-supernatants were subjected to ultracentrifugation (Beckman-Coulter) (115,000×*g*, 60 min, 4 °C) to enrich for a membrane protein fraction. The pellets containing the EMFs were washed in a 50 mM Tris–HCl buffer (pH 8.0) and ultracentrifuged twice (115,000×*g*, 30 min, 4 °C) to remove the enrichment buffer. The final EMFs were solubilized in 1 ml of solubilization buffer containing 7 M urea, 2 M thiourea, 2% CHAPS, 10% isopropanol, and protease inhibitor cocktail, with an optional addition of 0.5% bromophenol blue to visually assess the integrity of protein isolation. Protein concentrations of the samples were determined using a 2D-Quant Kit (GE Healthcare), and the samples were aliquoted and frozen at −20 °C until further use.

Author Manuscript Author Manuscript Author Manuscript Author Manuscript

2.5. B. pertussis immune sera

Three-week-old female BALB/C mice were initially injected intraperitoneally (i.p.) with 1×10^9 colony forming units (cfu) of T, C, D, or F suspended in 10 μl of physiological saline (pH 7.2). Before injection, strains were cobalt-irradiated using 5×10^6 γ RAD to inhibit bacterial replication and infectivity, while preserving bacterial surface structures. The process was repeated 2 weeks later, every 2 weeks thereafter, with three separate i.p. immunizations of similar dosage for 6 weeks. At this time, mice were euthanized according to AALAC and IACUC standards and the *Bp* immune sera generated from each strain were collected from blood. The collected serum was aliquoted and stored at −70 °C until use. Additionally, a serum pool composed of sera drawn from convalescent pertussis human patients obtained from the CDC Pertussis Laboratory was used in this analysis. This pool is the Pertussis Laboratory ELISA standard reference sera acquired in accordance with CDC Institutional Review Board standards and regulations.

2.6. 1D sodium dodecyl sulfate-polyacrylamide gel electrophoresis (SDS-PAGE) and immunoblot analysis of B. pertussis EMF

Unless specified, materials, antibodies, and procedures for GE and immunoblot analysis were obtained from Bio-Rad (Hercules, CA, USA). 10 μg of total EMF proteins from each strain was suspended in Laemmli sample buffer and electrophoresed on 12.5% SDS-PAGE gels following standard protocols (Laemmli, 1970). To visualize separated proteins, gels were stained using the hot coomassie blue staining protocol. EMF proteins were electroblotted (Towbin et al., 1979) onto polyvinylidene fluoride (PVDF) membranes for 1 h and probed with either a primary *Bp* strain-specific immune or preimmune (normal) mouse serum. Immunoreactive bands were further probed with a secondary goat-anti-mouse horseradish peroxidase-conjugated IgG antibody and subsequently visualized with 1,4-benzenediamine dihydrochloride (Sigma-Aldrich).

2.7. PVDF on-membrane protein extraction

Protein extraction directly from blotted-PVDF membranes was performed based on Bienvenut et al. (1999), but modified accordingly. PVDF membrane bands containing EMF proteins from T and C associated with immunoreactivity were excised and destained with 50% methanol (500 μl) for 2 h at room temperature (RT). After destaining, the supernatant was removed. The membrane pieces were air dried, followed by the addition of 50 mM ammonium bicarbonate ($NH_4(CO_3)_2$) digestion buffer in 30% acetonitrile (ACN) (Fisher Scientific). The protein-containing membrane pieces were then incubated overnight (ON) with trypsin (0.1 μg/μl) (Promega Corporation, Carlsbad, CA, USA) at 37 °C. After digestion, the supernatant was collected and the membranes were treated with 80% ACN to extract the peptides and sonicated at level nine (Aquasonic™ model 150-D)(VWR Scientific Products, Suwanee, GA) for 15 min. Following sonication, the extract was pooled with the previous supernatant, dried via vacuum centrifugation, and resuspended in dH_2O (50 μl). Samples were prepared for nLC-ESI-MS/MS, in which peptides were suspended in equal volumes of 0.1% formic acid.

Author Manuscript Author Manuscript Author Manuscript Author Manuscript

2.8. EMF protein identification

T, C, D, or F EMFs (10 μg) before direct proteolytic cleavage were treated with 0.1% rapigest (RG) (Waters Corporation, Milford, MA, USA) in $NH_4(CO_3)_2$ digestion buffer at 100 °C for 5 min to denature proteins. Upon cooling at RT, the samples were incubated ON with trypsin (10 μg) (Promega) at 37 °C. After incubation, the RG was inactivated in the presence of 1 M HCl for 30 min at 37 °C, and centrifuged at 12,000×*g* for 15 min. The supernatant was removed and suspended in equal volumes of 0.1% formic acid and analyzed by nLC-ESI MS/MS. The data obtained represent two distinct biological preparations, each performed in triplicate.

2.9. Immunoprecipitation studies using antibody affinity magnetic bead capture technology

Dynal beads (Invitrogen Corporation, Carlsbad, CA, USA) coated with protein G for immunoglobulin (IgG) capture and subsequent immunoprecipitaton (IP) of EMFs were used as per the manufacturer's recommendation with the following changes. The Dynal beads (200 μl per sample) were initially washed three times via resuspension in 800 μl phosphate citrate buffer (PCB), pH 5.0 (Sigma-Aldrich). Next, the beads were resuspended in 800 μl PCB and incubated ON at 37 °C in the presence of immune sera (100 μg total) from mice immunized against T, C, D or F. We also prepared controls containing normal mouse immune sera (100 μg total) and beads only. After incubation, the beads were magnetically stabilized, the supernatant was removed, and the beads were washed two times with 2 M triethanolamine, pH 8.2 (Sigma-Aldrich). This was to remove unbound antibodies and to equilibrate the beads for antibody crosslinking. The immune-sera bound beads were next cross-linked with 1 ml 20 mM dimethyl pimelimidate (Sigma-Aldrich) in 2 M triethanolamine for 30 min at RT via inversion. Following crosslinking, the beads were washed two times in 800 μl phosphate buffer saline (PBS), pH 7.0 with 0.1% Tween 20 and further incubated with 800 μl TBE (Sigma-Aldrich) to reduce non-specific (NS) protein binding. The beads were resuspended in 50 μl dH_2O. Then they were incubated at 37 °C ON in the presence of T, C, D or F EMFs (10 μg) that corresponded with the bead-Ab source strain (e.g., beads bound with T-specific IgG were incubated in the presence of T-EMF). After magnetic stabilization, the beads were washed via a mixer three times for 5 min with 100 μl PBS at RT to remove any unbound or NS-bound EMF proteins. The protein-bound Ab-coupled complexes were resuspended in 50 μl $NH_4(CO_3)_2$ digestion buffer treated with 0.1% RG followed by ON trypsin (10 μg) digestion at 37 °C.

Upon incubation, the IP complex was magnetically stabilized, and the supernatant containing EMF tryptic peptides was transferred to a fresh tube and dried via vacuum centrifugation to concentrate samples. The RG was inactivated and the samples prepared for nLC-ESIMS/MS, in which peptides were suspended in equal volumes of 0.1% formic acid. The data represent two biological preparations, each performed in duplicate. Simultaneously, Dynal beads were conjugated with pooled human convalescent sera (100 μg total) resulting from *Bp* infection in addition to normal human IgG (Interstate Blood Bank, Inc., Memphis, TN, USA). The IgG bound-beads were incubated with T, C, D, or F EMF (10 μg), and the samples were processed as described above.

Author Manuscript Author Manuscript Author Manuscript Author Manuscript

2.10. Nano liquid chromatography electrospray ionization mass spectrometry

Protein identification was achieved by using nanoflow liquid chromatography (nano-LC), data-dependent tandem mass spectrometry, and database searching. A pulled-needle, fused silica capillary (365 μm O.D. by 75 μm I.D.) (New Objective, Inc., Woburn, MA) was packed with 10 cm of 5 μm Symmetry 300 reverse-phase packing material (Waters Inc., Bedford, MA). Protein digests were loaded onto the analytical column and separated by gradient elution using an Eksigent 2D nanoLC system (Eksigent Technologies, Inc, Dublin, CA). The mobile phase solvents consisted of (solvent A) 0.2% formic acid (Thermo Scientific, Rockford, IL), 0.005% trifluoroacetic acid (Sigma-Aldrich) in water (Burdick and Jackson, Muskegon, MI), and (solvent B) 0.2% formic acid, 0.005% trifluoroacetic acid in acetonitrile (Burdick and Jackson). The gradient flow was set at 400 nl/min. The profile consisted of a hold at 5% B for 5 min followed by a ramp to 30% B over 100 min, then a ramp up to 90% B in 5 min and a hold at 90% for 2 min before returning to 5% B in 2 min and re-equilibration at 5% B for 20 min. After chromatography, peptides were introduced into an LTQ Orbitrap tandem mass spectrometer (Thermo Scientific, San Jose, CA). A 2.0 kV voltage was applied to the nano-LC column. The mass spectrometer was programmed to perform data-dependent acquisition by scanning the mass range from mass-to-charge (m/z) 400 to 1600 at a nominal resolution setting of 60,000 for parent ion acquisition in the Orbitrap. Most tryptic peptides fall within the stated m/z range and served as the basis for this selection. For MS/MS analysis the mass spectrometer chose the top 10 most intense ions with two or more charges. Singly charged ions were rejected for MS/MS as these ions are likely due to detergents or other sample additives. In particular for a data-dependent acquisition, time is better utilized acquiring for doubly and triply charged amino acids, which predominantly have greater sequence specificity since they are larger peptides and thus provide a higher likelihood in which to uniquely identify a protein.

All tandem mass spectra were extracted from the raw data file using Mascot Distiller (Matrix Science, London, UK; version 2.2.1.0) and searched using Mascot (version 2.2.0). Mascot was set up to search using the entire NCBInr database or a modified NCBInr database created to search "*Bordetella*"- or "pertussis"- recognized proteins in which trypsin is used as the digestion agent. Mascot was searched with two missed cleavages, a fragment ion tolerance mass of 0.80 Da, and a parent ion tolerance of 200 ppm, while oxidation was selected as a variable modification. Scaffold (Proteome Software, Portland, OR) was used to validate MS/MS based peptide and protein identifications.

Peptide identifications were accepted if they could be established at greater than 95.0% probability as specified by the Peptide Prophet algorithm (Keller et al., 2002). Protein identifications were accepted if they could be established at greater than 99.0% probability and contained at least two identified peptides (Nesvizhskii et al., 2003). With these stringent parameters of Peptide Prophet and Protein Prophet within the Scaffold software, the probability of a wrong assignment is below 0.1%. PSORTb subcellular scores were used to predict and localize identified EMF proteins (http://www.psort.org/psortb/) (Yu et al., 2010). Lastly, KEGG identifiers using NCBI Gi accession numbers were employed to assign functions to each of the identified proteins http://www.genome.jp/kegg/kegg3.html (Tefon et al., 2011).

Author Manuscript Author Manuscript Author Manuscript Author Manuscript

3. Results

3.1. 1GE and immunoblot analysis of B. pertussis species EMFs

Carbonate-enriched EMF proteins were initially separated by 1D-SDS-PAGE (1D-GE). This was to observe common and differential banding patterns between the T-reference strain and clinical isolates C, D, and F. Overall, similar protein profiles among the strains were observed, with 1D-GE revealing slight differences and no unique protein banding patterns between the strains (Fig. 2). Subsequently, after observing no major protein differences, we used classical immunoblotting approaches to assess the strain's ability to invoke an immune response in vivo. EMF-transferred PVDF membranes, probed with strain-specific mouse antisera, showed comparable patterns of immunoreactivity between all four strains. Likewise, the similarity in the immunoblot corresponded with the heavy banding patterns between 30 and 70 kDa observed in the stained gel (data not shown).

Collectively, the gel and immunoblot results indicate similarity in the proteins expressed among these strains. And nominal differences appeared between the immune responses seen in mice against T, C, D, and F. Nevertheless, to delineate any significant variability which was not visually observable, a few major immunoreactive protein bands from 30 to 35 and 40 to 45 kDa were analyzed for T and C. Peptides extracted from tryptically digested, excised-PVDF membranes were separated and analyzed using nLC-ESI-MS/MS. Database mining revealed a few proteins in both the T and C highly immunoreactive bands. These included a 42-kDa outer membrane porin precursor (OmpP), a 40-kDa outer membrane porin protein OmpQ (OmpQ), and a 40-kDa putative exported protein. The C-EMF-probed excised protein bands also identified a 33-kDa putative membrane protein.

3.2. Direct surfaceome analysis of Bp EMFs using nLC-ESI-MS/MS

Although *Bp* EMF proteins were separated and visualized using GE, and a few further identified by an on-membrane analysis in combination with MS, a more direct and less time-consuming surfaceome analysis was ultimately implemented.

RG-treated and trypsinized-EMFs from the four strains were analyzed directly using nLC-ESI MS/MS. This was followed by database searching, in which 259, 249, 253, and 245 proteins were identified for T, C, D and F, respectively. However, based on greater than 95% Scaffold protein identification and amino acid coverage probabilities, 193 total proteins among all four strains were further selected (Table 2A). Moreover, using PSORTb subcellular localization scores, proteins considered membrane (outer, periplasmic, or cytoplasmic) or found in the cytoplasm accounted for 44% and 29%, respectively, of the total “surfaceome” identified in this study. The remaining proteins classified as “unknown” were possibly localized to the membrane or cytoplasm and comprised 27% of the total surfaceome (Table 2B).

In general, the identified proteins included, but were not limited to, secreted proteins and toxins, as well as outer membrane proteins affiliated with cell membrane synthesis, cellular transport, adhesion, pathogenesis, or virulence. Additionally, the EMF proteomic profiles consisted of proteins associated with protein synthesis. These included highly abundant

Author Manuscript Author Manuscript Author Manuscript Author Manuscript

ribosomal proteins and elongation factors, DNA synthesis-associated proteins, metabolic enzymes, and hypothetical proteins (HP) with unknown functions (Table 2C).

In all, we discovered 163 proteins in the EMFs of all four strains (Table 2D). Among them were the expected surface proteins filamentous hemagglutinin adhesin (FHA) and pertactin (Prn), OmpQ, a serum resistance protein (BrkA), a TonB-dependent receptor for iron transport (TonB), a tracheal colonization factor precursor (TcfA), 30S ribosomal proteins S2 and S3, chaperonin GroEL (GroEL), and elongation factor Tu (EF-Tu). Common proteins were also identified in a combination of two or three strains and absent in the remaining. Other proteins were detected only in T while absent in C, D, and F, including CTP synthetase, HP *Bp* 1123 and, a putative ketopantoate reductase among others. Conversely, proteins were detected exclusive to C, D, and F while not present in T, such as a putative periplasmic solute-binding protein. Lastly, proteins were identified exclusively to C, D, or F. These included HP *Bp* 3441, a trigger factor, and an exopolyphosphatase, respectively (Table 2D).

3.3. Direct putative immunoreactive protein identification using nLC ESI-MS/MS

To identify putative antigenic proteins directly from the EMFs and to ascertain any differential immunoreactive proteomic profiles among the four strains, antigen-antibody (Ag-Ab) affinity capture technologies were employed. Trypsin-digested EMF proteins immunoprecipitated with coupled magnetic-bead strain-specific mouse antisera were analyzed via nLC-ESI MS/MS. Among each of the strains T, C, D, and F, 19, 31, 31, and 12 total “putative immunogenic proteins” (PIPs) were identified by database search analysis, respectively (Table 3A). Of the 48 total distinct PIPs detected between all 4 strains, 50% were membrane-associated with 60% of these proteins localized to the outer membrane and/or extracellular. The remaining 24 PIPs, accounting 23% and 27% were localized to the cytoplasm or of unknown location, respectively. For example, Prn, TonB, GroEL, EF-Tu, and a putative sulfatase were some of the proteins identified among all the strains (Table 3B). Collectively, the common PIPs (bold-black outlined box) detected in all T, C, D, and F strains were OmpQ, OmpP, putative lipoprotein, OmpA, BrkA, TcfA, and HP *Bp* 1440. Alternatively, a Vag8 autotransporter, preprotein translocase SecD (SecD), a putative peptidoglycan-associated protein, SCO1/SencC family and a thiol:disulfide interchange protein (DsbA) were identified in only C, D, and F (blue shaded box) and not detected in the T-EMF/Ab immunoprecipitated complex. Five, 11, and 9 strain-specific PIPs were detected in the T-, C- and D-EMF Ab-bead complexes. Included among those were HP *Bp* 0455, a putative inner membrane protein, and a putative bifunctional protein, respectively (Table 3B). No strain-specific PIPs were detected in the F-EMF/Ab IP complex. It is worth noting that varying degrees of cross-reactivity (CR) or nonspecific (NS) interactions were generated (denoted with an asterisk) using stable IP between the strains' EMF to the normal mouse IgG-bound bead control. And these interactions can be reasonably explained from a biological perspective as depicted in Fig. 3. TcfA, OmpP, and OmpA with evident cross reactivity were discovered in all 4 strains. Furthermore, the total PIPs correlating to mouse pertussis immunity comprised 11, 18, 18, and 7% of total T, C, D, and F surfaceome proteomic profiles, respectively (Table 3A). But taking any tentative cross-reactivity into

Author Manuscript Author Manuscript Author Manuscript Author Manuscript

consideration, subtracting the nonspecific interactions from the total number of PIPs resulted in a 23–39% reduction of more probable antigenic candidates.

Finally, we performed a MS-based immunoproteomic study using coupled magnetic bead-pooled human convalescent serum in combination with EMFs. This was to identify novel antigenic proteins that potentially correlate with human response to pertussis infection. The study, as summated in Tables 4A and 4B, revealed that human antibodies contained in the pooled serum immunoreacted with 4, 12, 8, and 10 proteins present in T-, C-, D-, and F-EMFs, respectively. Moreover, of the 15 total distinct PIPs detected by nLC-ESI MS/MS among all 4 strains, more than half were extracellular or localized to the outer membrane, including Vag8, BrkA, and TonB. Five proteins: HP *Bp* 0205, HP *Bp* 1485, HP *Bp* 3689, a probable inner membrane, and TonB revealed strain-specific detection in the human IP. Only two – a probable inner membrane protein and HP *Bp* 3689 – were unique to C and F, respectively. Once again, accounting for any non-specific interactions between normal human IgG antibodies and the EMFs, the pool of PIPs identified in this foundational assessment is diminished to 1, 3, 0, and 5 for T, C, D, and F, respectively. Lastly, in both the mouse and human immunoproteome examinations, 14 proteins were commonly identified, of which OmpQ and OmpA were the only proteins detected in all four immune complexes.

4. Discussion

In spite of widespread vaccination, disease caused by *Bp* is rapidly increasing in the United States. In this pilot study we compared the proteomes of one past *Bp* strain with three current circulating strains in which any subtle changes in their proteome profile could have pathogenic and immunological implications. Additionally, we employed a non gel-based technique to compare surface proteins and immunoproteins from the four *Bp* strains. Previous studies of bacterial surfaceomes for the identification of clinical diagnostic biomarkers (and more so, novel vaccine candidates) have all incorporated approaches that involve to a certain extent subproteome fractionation and gel-based separation followed by MS and protein identification (Thein et al., 2010). Our initial path of study in characterizing the surfaceomes of three recent *Bp* circulating isolates and one older isolate from 1954 began with a 1D-GE EMF protein assessment. This revealed no major protein banding differences or unique patterns. In an effort to maximize protein discovery, however, we implemented a gel-free surfaceome profiling approach. This proved advantageous and fruitful in identifying total proteins and was in partial concurrence with previous *Bp* surfaceome analysis.

Bottero et al. (2007) described a comparative surfaceome analysis of 3 *Bp* vaccine producing strains. The methodology included T and an Argentinean clinical isolate 106, in which 54 total proteins from enriched *Bp* surface extracts were identified using 2D-GE in parallel with matrix-assisted laser desorption ionization-time-of-flight (MALDI-TOF) MS analysis.

In our direct nLC-ESI MS/MS *Bp* surface assessment, 139 more proteins were identified than in the gel-based Bottero study (Bottero et al., 2007). Bottero similarly identified 21 of the total 193 proteins, of which approximately 40% of this subset localized to the outer membrane. These included a competence lipoprotein, FHA, OmpQ, OmpP, OmpA, Prn,

Author Manuscript Author Manuscript Author Manuscript Author Manuscript

BrkA, and a putative quino protein. Among the cytoplasmic proteins, both studies discovered a capsular polysaccharide biosynthesis protein, putative L-lactate dehydrogenase, GroEL, and EF-Tu. And as summated in Table 2D, the remaining 172 proteins identified in our study were localized to the membrane or cytoplasm. They either “moonlight” (perform multiple cellular roles), serve in a cellular housekeeping capacity such as energy production, or engage in membrane-associated activities such as biogenesis, adhesion, or transport.

Our surfaceome profile resulted in a higher number of proteins identified. Given that our preparation is enriched and not exclusive for the surface membrane, more nonsorted cytoplasmic proteins may have been retained in the fraction compared with Bottero's enrichment method, thus resulting in more proteins in the starting material. Additionally, the profile generated is a direct analysis of a conformationally native in-solution protein pool versus a protein-embedded, gel excised spot or band. Consequently, this state would ideally allow proteolytic enzymes greater accessibility to the protein itself and result in a potentially higher yield of peptides generated by tryptic digestion. MALDI-TOF is a fruitful MS technology, in particular for its speed in analyzing a sample, but generally in terms of accuracy, peptide capacity, peptide resolution, and detection sensitivity, the nLC-ESI MS/MS used in our study is more advantageous and lends itself to higher numbers of proteins identified.

Other factors such as database annotation, peptide ionization potential, subproteome extraction, and protein abundance can also affect the success of protein identification. First, the *Bp* clinical isolates used in these studies have yet to be sequenced and thus are not present in the database. Therefore, some MS/MS data may not be matched to proteins in the existing database, resulting in lower protein discovery. Also, as in the case for both studies, due to amino acid composition (i.e., hydrophobic peptides) some peptides do not ionize well. Thus, their abundance may not be enough to trigger the mass spectrometer to conduct an MS/MS experiment. And some peptides may not fragment efficiently, leading to complete inability for the searching algorithm to match the data to the protein, irrespective of the MS instrumentation used. Again, due to chemical composition of the proteins and the extraction buffers utilized, some proteins may even be lost in the preparation (Bottero et al., 2007; Altindis et al., 2009). Note too that proteins commonly identified between both studies are cellularly abundant (i.e. EF-Tu) and large in molecular weight (i.e., FHA). Consequently, when these proteins are enzymatically digested they will likely generate more peptides that would have a greater propensity of detection. This could hinder the detection of smaller proteins, which obviously would have fewer tryptic peptides. Though our direct, gel-free, EMF nLC-ESI MS/MS analysis may require optimization of extraction steps to ensure a greater retention of outer membrane proteins and reduce “contamination” by abundant cytoplasmic proteins that may overshadow less abundant proteins, the approach can be used to examine other *Bp* circulating isolate surfaceomes for novel surface-expressed protein discovery.

The next phase of our study moved from elucidating what proteins comprised the enriched surfaceome to what proteins actually have the ability to induce an Ab-mediated response. We deviated from classical immunoblotting techniques, such as those used by Altindis et al. (2009), for a less-labor intensive, more rapid Ag–Ab affinity approach. The Ag–Ab method

Author Manuscript Author Manuscript Author Manuscript Author Manuscript

has an added benefit of identifying surface proteins with both continuous and noncontinuous epitopes while immunoblotting techniques generally can only probe continuous epitopes. Today, conjugated Ab-magnetic bead capture technologies are widely used for protein IP. Generally, protein G-coated magnetic Dynal™ beads capture from antisera IgG populations traditionally associated with direct Ab-mediated immune responses. This Ab-bead complex is immunoprecipitated or “pulled down” with proteins, if immunostimulatory would uniquely “match” and interact with its specific Ab. Once the protein-Ab-bead complex is pulled-down and washed to remove nonspecific binding, the beads are subjected to enzymatic digestion by trypsin and the peptides are analyzed by nLC-MS/MS. The respective proteins are identified by database searching.

Kudva et al. (2005) used this Ab-bead capture technology to identify anthrax spore surface proteins in response to human anthrax vaccine adsorbed-induced immunity. Here we similarly describe the use of Ag–Ab affinity for stable IP of *Bp* EMFs using strain-specific mouse-antisera, and couple this technique to MS to identify novel putative antigenic proteins. Of the 48 total proteins detected among our strains, 10 well-known immunogens were identified, including Vag8, GroEL, Prn, BipA, serotype 3 fimbrial subunit (Fim3), BrkA, OmpQ, OmpP, OmpA and TcfA (van den Berg et al., 1999; Oliver and Fernandez, 2001; Fuchslocher et al., 2003; Elder and Harvill, 2004; Matoo and Cherry, 2005; Zhu et al., 2010). The latter five are commonly detected in all four strains. Other known *Bp* immunogens such as Ptx, FHA, Dnt, Fim2, or CyaA, the latter four identified in our total surfaceome profile, may have been immunoprecipitated and, due to peptide composition, simply not detected by MS. EF-Tu, EF-Ts, glyceraldehyde-3-phosphate dehydrogenase (Gdh), and a putative L-lactate dehydrogenase (Ldh) are immunogens commonly conserved in other pathogens (Zhu et al., 2010; Chitlaru et al., 2007; Ling et al., 2004) were also identified in our *Bp* affinity capture assessment. Additionally, Altindis et al. (2009) used strain-specific mouse antisera to perform a 2D-GE immunoproteomic study aimed at identifying novel immunogens in T and in the *Bp* Saadet strain, a 1948 Turkish isolate. The Altindis study discovered 25 total proteins, of which EF-Tu, Prn, BrkA, and ketol-acid reductoisomerase were comparably identified in all or some of the isolates in our examination. Even more, Tefon et al. (2011) described an extension of the 2009 Altindis study using 2D-GE in parallel with nLC-MS/MS to identify 11 more immunogens of *Bp* T and the Saadet strain, of which three – Prn, GroEL and BrkA – were, as stated, discovered in our study.

Identification of more similar proteins from the Altindis and Tefon studies is likely dependent on differential method design. Nevertheless, these proteins, along with the OmpP and OmpQ comparably identified in both our pilot immunoblot and IP study, in addition to the other known antigen identifications are confirmation that the capture technology is a fruitful alternate approach available for *Bp* immunogen discovery.

Of the remaining PIPs determined as common among T, C, D, and F, HP *Bp* 1440 and a putative lipoprotein are both possibly associated with transport and adhesion and could be considered as novel putative *Bp* antigens. Moreover, of the 5 PIPs only detected in the recent circulating C, D, and F isolates, only Vag8 was previously identified as immunogenic. The putative peptidoglycan associated-lipoprotein, SCO1/SenC family protein, DsbA, and SecD

Author Manuscript Author Manuscript Author Manuscript Author Manuscript

are proteins involved in outer membrane lipid attachment; membrane biogenesis and cytochrome c assembly, protein turnover, protein folding and energy production; and membrane protein secretion and export, respectively (Parkhill et al., 2003). Note too that their unique identification to the clinical strains could provide insight into the overall immunopathogenesis of past and recent pertussis cases.

Even more, immunogen screening via IP also identified PIPs unique to each strain. First, the T-EMF study detected five specific PIPs, one of which is BipA, a known immunogen. HP *Bp* 0455 and its *Bordetella bronchioseptica* (*Bb*) BB4955 homolog, both putatively associated with organic anion transport, also were identified (Parkhill et al., 2003), as were a putative inner membrane protein (*Bp* 3326) and a surface antigen, similar to the outer membrane protein assembly complex YaeT.

Second, the C-EMF study detected 11 specific PIPs, which included previously identified immunogens EF-Ts, GDH, LDH, and ketolacid reductoisomerase. Fructose 1-6-bisphosphate aldolase (Fba), N-acetyl-gamma-glutamyl-phosphate reductase (ArgC), and phosphor-2-dehydro-3-deoxyheptonate aldolase (AroG) are all metabolic enzymes involved in glycolysis, gluconeogenesis, or amino acid biosynthesis (Parkhill et al., 2003; Matoo and Cherry, 2005). Two proteins, similar to the bacterial, extracellular solute-binding protein family 7, exported solute-binding and periplasmic solute-binding (SmoM) were also found to be immunostimulatory (Parkhill et al., 2003; Matoo and Cherry, 2005). A rod-shape determining protein associated with the MreBCD complex was also identified.

Third, the D-EMF study detected nine specific PIPs, which included HP BP1057—a protein similar to *E. coli* Elab. A putative bifunctional protein, a metabolic protein similar to *P. aeruginosa* cytochrome c oxidase, and a F0F1 ATP synthase subunit B (an enzyme part of the membrane proton pump involved in ATP synthesis) were discovered. A probable *Bp* inner membrane protein and its homologous *Bb* translocase YidC, a membrane insertase, were identified as immunoreactive. A putative peptidase, associated with bacterial wall degradation and a signal peptidase I – an enzyme similar to the essential membrane bound serine protease leader peptidase B – were uniquely immunoprecipitated in the D antibody/EMF complex. A putative sulfatase containing phosphoglycerol transferase activity-like domains possibly associated with cell envelope biogenesis, was also discovered. Protective antibodies, for instance generated against this sulfatase, if not expressed in humans, could potentially impair bacterial cell growth and ultimately reduce infectivity and transmission of pertussis. Lastly, of the 14 PIPs identified in F, none were unique to this isolate.

Moreover, with differential and lower immunoreactivity among the strains, as in the case with strain F, one may wonder why variation exists and the usefulness of strain-specific PIPs as potential candidates for clinical diagnostics and improved vaccine development. First, an important reminder is that *Bp* T is a lab-adapted strain in which virulence observed over the years may have weakened, reducing its immunopotency and contributing to fewer PIPs identified.

Author Manuscript Author Manuscript Author Manuscript Author Manuscript

Second, C, D, and F strains all were isolated in different U.S. geographical regions between 1998 and 2007 and presumably from different individuals, thus, the identification of unique, strain-specific PIPs is not unlikely. Also, although *Bp* T, C, D, and F OMP extraction and enrichments were performed under the same conditions and time, some proteins exhibiting antigenic properties might have been lost during the preparation process. Nevertheless, regardless of strain differences, all the aforementioned PIP biological roles could prove insightful into the overall immunopathogenesis of *Bp* and provide a greater epidemiological understanding of pertussis incidence and how better to diagnose, treat, and – most importantly – prevent the disease.

As alluded, though specific Ag–Ab interactions were formed and measures taken in the method to reduce nonspecific binding, cross-reactivity of strain-specific Ags from the EMFs to normal mouse IgG-bound bead controls was observed. Proteins commonly immunoprecipitated in all strains, such as OmpQ and OmpA, exhibit cross-reactive or nonspecific tendencies and are reasonably explained from a biological perspective (Fig. 3). First, the EMF protein interactive with the Ab-bead in its natural state exists as a complex. Second, because not all of the available sites on the protein G-beads will be occupied by IgG-specific antibodies, *Bp* proteins present in the EMF with biochemical properties that allow for interaction directly to the protein G could exist. Third, *Bp* proteins could nonspecifically bind to glycoprotein-antibody moieties. Also, cross-reactivity may simply persist due to protein abundance in which residual amounts of detectable protein remain even after several washes upon IP and before protein digestion. Under all of these scenarios, upon tryptic digestion not only the bound specific protein is digested, but also those making up complex formations are digested as well, all of which could be simply considered as nonspecific. With all that said, regardless of the origin of cross-reactivity, identified immunogens are merely putative. To be considered true candidates as biomarkers for clinical diagnostics and improved vaccine development, they have to be validated extensively on a proteomic level and, most importantly, in vivo.

Information gained from immunoproteomic studies that use *Bp*-generated mouse antisera as the basis for novel immunogen discovery are quite valuable to identify possible immunoreactive proteins. But individual, *Bp*-stimulated human antibody or pooled serum from actively infected or even convalescent pertussis patients is more ideal and provides a more relevant immunological perspective of human pertussis infection. In our study, 15 total PIPs among T, C, D, and F were recognized by pooled human antibodies from patients recovering from pertussis infection—a more than 3-fold reduction in total PIPs identified using the mouse model. Moreover, strain-specific antisera generated from whole inactivated *Bp* T, C, D, and F from immunized animals versus a pooled serum from convalescent pertussis-infected human patients are a clear factor that may play a role in differential immunoreactivity. Although not comparable with methodologies performed in our study, Zhu et al. (2010) recently described a 2D-GE proteomic assessment of total *Bp* membrane enriched and extracellular protein preparations. The purpose was to investigate the complete set of *Bp* antigenic proteins using antisera generated in response to Chinese whole-cell, vaccine-induced immunity.

Author Manuscript Author Manuscript Author Manuscript Author Manuscript

In the Zhu study, twice as many total immunogens were identified for human sera compared with our human sera pool. The disparity was possibly due to *Bp* strain differences and lower post-pertussis infection specific circulating Ab titer levels of the pooled human antisera (caused by prior serum dilution) used in our study. Interestingly, irrespective of the subproteome extraction, protein enrichment, and immunodetection methods used, OmpQ was the only protein pulled down using both mouse and human antisera from all four *Bp* EMFs in our study, as well as in Zhu's immunoproteomic examinations.

In conclusion, we used Ag–Ab affinity capture technologies in conjunction with MS to identify immunoreactive proteins in three recent circulating *Bp* strains. The overall goals were to identify biomarkers that could be evaluated for use in pertussis strain differentiation and in clinical diagnostics, and to detect novel targets for design of prevention and therapeutic strategies.

As a first step in this qualitative proteomics study, we examined the applicability of a gel-free direct enzymatic-treated *Bp* EMF surfaceome analysis. Common and strain-specific surface expressed protein profiles compared to the current vaccine-producing T strain were generated, suggesting that there may be subtle differences of surface protein expression among *Bp* strains. Further characterization of these differentially expressed proteins at the molecular level is warranted; which may reveal minor changes that could have implications on virulence and pathogenesis.

Second, antibodies generated from pertussis interperitoneal mouse inoculation were used to assess protein immunogenicity and revealed the identification of known and unknown *Bp* antigens using a stable IP approach. A comprehensive proteomic examination and an in vivo immunopotency assessment are further needed to validate these PIPs as true biomarker and vaccine candidates. Also, reassessing the immunoproteome of our unique *Bp* strains by stable IP using several human sera from active pertussis infected human patients will provide a more consistent depiction of the pertussis immunoproteome. Additionally, efforts to enhance novel immunogen discovery may require immunodepletion of known and highly abundant antigenic-specific antibody populations, such as OmpQ and BrkA. Highly abundant antigenic proteins would in essence generate a larger specific IgG antibody pool. This larger antibody subset would have a greater chance of binding to protein G-beads, which invariably could overshadow lower expressed immunostimulatory proteins.

Nonetheless, the gel-free approach described here for immunoproteome identification remains a fruitful alternative for antigen discovery. And because this is a pilot study using a small number of temporally limited and genetically diverse strains, future studies will entail using the described methods to examine a larger set of epidemiologically significant strains with these putative, novel candidates laying the foundation for clinical diagnostic design and improved vaccine development, leading to the ultimate prevention of this deadly infection.

4.1. Disclaimer

References in this article to any specific commercial products, process, service, manufacturer, or company do not constitute an endorsement or a recommendation by the U.S. Government or the Centers for Disease Control and Prevention. The findings and

Author Manuscript Author Manuscript Author Manuscript Author Manuscript

conclusions in this report are those of the authors and do not necessarily represent the views of CDC.

References

Advani A, Donnelly D, Hallander H. Reference system for characterization of *Bordetella pertussis* pulsed-field gel electrophoresis profiles. J. Clin. Microbiol. 2004; 42(7):2890–2897. [PubMed: 15243034]

Altindis E, Tefon BE, Özcengiz Y, Becher D, Hecker M, Özcengiz G. Immunoproteomic analysis of *Bordetella pertussis* and identification of new immunogenic proteins. Vaccine. 2009; 27:542–548. [PubMed: 19028538]

Bart MJ, van Gent M, van der Heide HG, Boekhorst J, Hermans P, Parkhill J, Mooi FR. Comparative genomics of prevaccination and modern *Bordetella pertussis strains*. BMC Genomics. 2010; 11(627):1–10. [PubMed: 20044946]

Bienvenut WV, Sanchez JC, Karmime A, Rouge V, Rose K, Binz PA, Hochstrasser DF. Toward a clinical molecular scanner for proteome research: parallel protein chemical processing before and during western blot. Anal. Chem. 1999; 17(21):4800–4807.

Bordet J, Gengou O. Le microbe de la coqueluche. Ann. Inst. Pasteur. 1906; 20:48–68.

Bottero D, Gaillard ME, Fingermann M, Weltman G, Fernandez J, Sisti F, Graieb A, Roberts R, Rico O, Rios G, Regueira M, Binsztein N, Hozbor D. Pulsed-field gel electrophoresis, pertactin, pertussis toxin S1 subunit polymorphisms, and surfaceome analysis of vaccine and clinical *Bordetella pertussis* strains. Clin. Vaccine Immunol. 2007; 14:1490–1498. [PubMed: 17699837]

Chen G, Prama BN. LC-MS for protein characterization: current capabilities and future trends. Expert Rev. Proteomics. 2008; 5:435–444. [PubMed: 18532911]

Chitlaru T, Gat O, Grosfeld H, Inbar I, Gozlan Y, et al. Identification of in vivo-expressed immunogenic proteins by serological proteome analysis of the *Bacillus anthracis* secretome. Infect. Immun. 2007; 75:2841–2852. [PubMed: 17353282]

Das P. Whooping cough makes global comeback. Lancet Infect. Dis. 2002; 2:322. [PubMed: 12144890]

Dreisbach A, Hempel K, Buist G, Hecker M, Cecher D, van Dijl JM. Profiling the surfaceome of *Staphylococcus aureus*. Proteomics. 2010; 10:1–15. [PubMed: 20043300]

Dworzanski JP, Snyder AP. Classification and identification of bacteria using mass spectrometry-based proteomics. Exp. Rev. Proteomics. 2005; 2(6):863–878.

Elder KD, Harvill ET. Strain-dependent role of BrkA during *Bordetella pertussis* infection of the murine respiratory tract. Infect. Immun. 2004; 72:5919–5924. [PubMed: 15385494]

Fuchslocher B, Millar LL, Cotter PA. Comparison of *bipA* alleles within and across *Bordetella* species. Infect. Immun. 2003; 71:3043–3052. [PubMed: 12761081]

Han X, Aslanian A, Yates JR III. Mass spectrometry for proteomics. Curr. Opin. Chem. Biol. 2008; 12:483–490. [PubMed: 18718552]

Hardwick TH, Cassiday P, Weyant RS, Bisgard KM, Sanden GN. Changes in predominance and diversity of genomic subtypes of *Bordetella pertussis* isolated in the United States, 1935 to 1999. Emerg. Infect. Dis. 2002; 8(1):44–49. [PubMed: 11749747]

He Q, Mertsola J. Factors contributing to pertussis resurgence. Future Microbiol. 2008; 3:329–339. [PubMed: 18505398]

http://www.cdc.gov/.

Hulbert RR, Cotter PA. Laboratory maintenance of *Bordetella pertussis*. Curr. Protoc. Microbiol. 2009; 15(4B):1.1–1.9. [PubMed: 19653214]

Jabbour RE, Wade MM, Desphande SV, Stanford MF, Wick CH, Zullich AW, Snyder AP. Identification of *Yersinia pestis* and *Escherichia coli* strains by whole cell and membrane protein extracts with mass spectrometry-based proteomics. J. Proteome Res. 2010; 9(7):3647–3655. [PubMed: 20486690]

Author Manuscript Author Manuscript Author Manuscript Author Manuscript

Keller A, Nesvizhskii AI, Kolker E, Aebersold R. Empirical statistical model to estimate the accuracy of peptide identifications made by MS/MS and database search. Anal. Chem. 2002; 74:5383–5392. [PubMed: 12403597]

King AJ, Berbers G, van Oirschot HF, Hoogerhout P, Knipping K, Mooi FR. Role of the polymorphic region 1 of the *Bordetella pertussis* protein pertactin in immunity. Microbiology. 2001; 147:2885–2895. [PubMed: 11700340]

Kudva IT, Griffin RW, Garren JM, Calderwood SB, John M. Identification of a protein subset of the anthrax spore immunome in humans immunized with the anthrax vaccine adsorbed preparation. Infect. Immun. 2005; 73(9):5685–5696. [PubMed: 16113286]

Kustos I, Kocsis B, Kilár F. Bacterial outer membrane protein analysis by electrophoresis and microchip technology. Expert Rev. Proteomics. 2007; 4(1):91–106. [PubMed: 17288518]

Laemmli UK. Cleavage of structural proteins during the assembly of the head of bacteriophage t4. Nature. 1970; 227:680–685. [PubMed: 5432063]

Lee EY, Choi DS, Kim KP, Gho YS. Proteomics in gram-negative bacterial outer membrane vesicles. Mass Spec. Rev. 2008; 27:535–555.

Ling E, Feldman G, Portnoi M, Dagan R, Overweg K, Mulholland F, Chalifa-Caspi V, Wells J, Mizrachi-Nebenzahl Y. Glycolytic enzymes associated with the cell surface of Streptococcus pneumoniae are antigenic in humans and elicit protective immune responses in the mouse. Clin. Exp. Immunol. 2004; 138:290–298. [PubMed: 15498039]

Litt DJ, Neal SE, Fry NK. Changes in genetic diversity of the *Bordetella pertussis* population in the United Kingdom between 1920 and 2006 reflect vaccination coverage and emergence of a single dominant clonal type. J. Clin. Microbiol. 2009; 47:680–688. [PubMed: 19158267]

Locht C. A common vaccination strategy to solve unsolved problems of tuberculosis and pertussis? Microbes Infect. 2008; 10:1051–1056. [PubMed: 18672086]

Matoo S, Cherry JD. Molecular pathogenesis, epidemiology, and clinical manifestations of respiratory infections due to *Bordetella pertussis* and other *Bordetella* subspecies. Clin. Microbiol. Rev. 2005; 18(2):326–382. [PubMed: 15831828]

Molloy MD. Isolation of bacterial cell membrane proteins using carbonate extraction. Methods Mol. Biol. 2008; 424:397–401. [PubMed: 18369877]

Nesvizhskii AI, Keller A, Kolker E, Aebersold R. A statistical model for identifying proteins by tandem mass spectrometry. Anal. Chem. 2003; 75:4646–4658. [PubMed: 14632076]

O'Farrell PH. High resolution two-dimensional electrophoresis of protein. J. Biol. Chem. 1975; 250:4007–4021. [PubMed: 236308]

Oliver DC, Fernandez RC. Antibodies to BrkA augment killing of *Bordetella pertussis*. Vaccine. 2001; 20:235–241. [PubMed: 11567769]

Parkhill J, Sebaihia M, Preston A, Murphy LD, Thomson N, Harris DE, et al. Comparative analysis of the genome sequences of *Bordetella pertussis*, *Bordetella parapertussis* and *Bordetella bronchioseptica*. Nat. Genet. 2003; 35:32–40. [PubMed: 12910271]

Poolman J, Hamstra HJ, Barlow A, Kuipers B, Loggen H, Nagel J. Outer membrane vesicles of *Bordetella pertussis* are protective antigens in the mouse intracerebral challenge model. FDA. 1990:202–206.

Singh M, Lingappan K. Whooping cough—the current scene. Chest. 2006; 130:1547–1553. [PubMed: 17099036]

Somner U, Peterson J, Pfeiffer M, Schrotz-King P, Morsczeck C. Comparison of surface proteomes of enterotoxigenic (ETEC) and commensal *Escherichia coli* strains. J Microbiol Methods. 2010; 83(2010):13–19. [PubMed: 20643167]

Taylor B, Fahm R. Pasteur Merieux Connaught five-component acellular pertussis vaccine. Biologicals. 1999; 27:103–104. [PubMed: 10600194]

Tefon B, MaaB S, Ozcengiz E, Becher D, Hecker M, Ozcengiz G. A comprehensive analysis of *Bordetella pertussis* surface proteome and identification of new immunogenic proteins. Vaccine. 2011; 29(19):3583–3595. [PubMed: 21397717]

Thein M, Sauer G, Paramasivam N, Grin I, Linke D. Efficient subfractionation of gram-negative bacteria for proteomics studies. J. Proteome Res. 2010; 9(12):6135–6147. [PubMed: 20932056]

Author Manuscript Author Manuscript Author Manuscript Author Manuscript

Towbin H, Staehelin T, Gordon J. Electrophoretic transfer of proteins from polyacrylamide gets to nitrocellulose sheets: procedure and some applications. Proc. Natl. Acad. Sci. U. S. A. 1979; 76:4350–4354. [PubMed: 388439]

van den Berg BM, Beekhuizen H, Mooi FR, van Furth R. Role of antibodies against *Bordetella pertussis* virulence factors in adherence of *Bordetella pertussis* and *Bordetella parapertussis* to human bronchial epithelial cells. Infect. Immun. 1999; 67:1050–1055. [PubMed: 10024542]

van Loo IH, Heuevelman KJ, King AJ, Mooi FR. Multilocus sequence typing of *Bordetella pertussis* based on surface protein genes. J. Clin. Micro. 2002; 40:1994–2001.

Wilkins, MR.Appel, RD.Williams, KL., Hochstrasser, DF., editors. Proteome Research: Concepts, Technology and Application. 2. Springer; Berlin: 2007.

Yu NY, Wagner JR, Laird MR, Mellj G, Rey S, Lo R, Dao P, Sahinalp SC, Ester M, Foster LJ, Brinkman FS. Improved protein subcellular localization prediction with refined localization subcategories and predictive capabilities for all prokaryotes. Bioinformatics. 2010; 26(13):1608–1615. [PubMed: 20472543]

Zhu YZ, Cai CS, Zhang W, Guo HX, Zhang JP, Ji YY, Ma GY, Wu JL, Li QT, Lu CP, Guo XK. Immunoproteomic analysis of human serological antibody responses to vaccination and whole-cell pertussis vaccine (WCV). PLoS One. 2010; 5(11):1–11.

Author Manuscript Author Manuscript Author Manuscript Author Manuscript

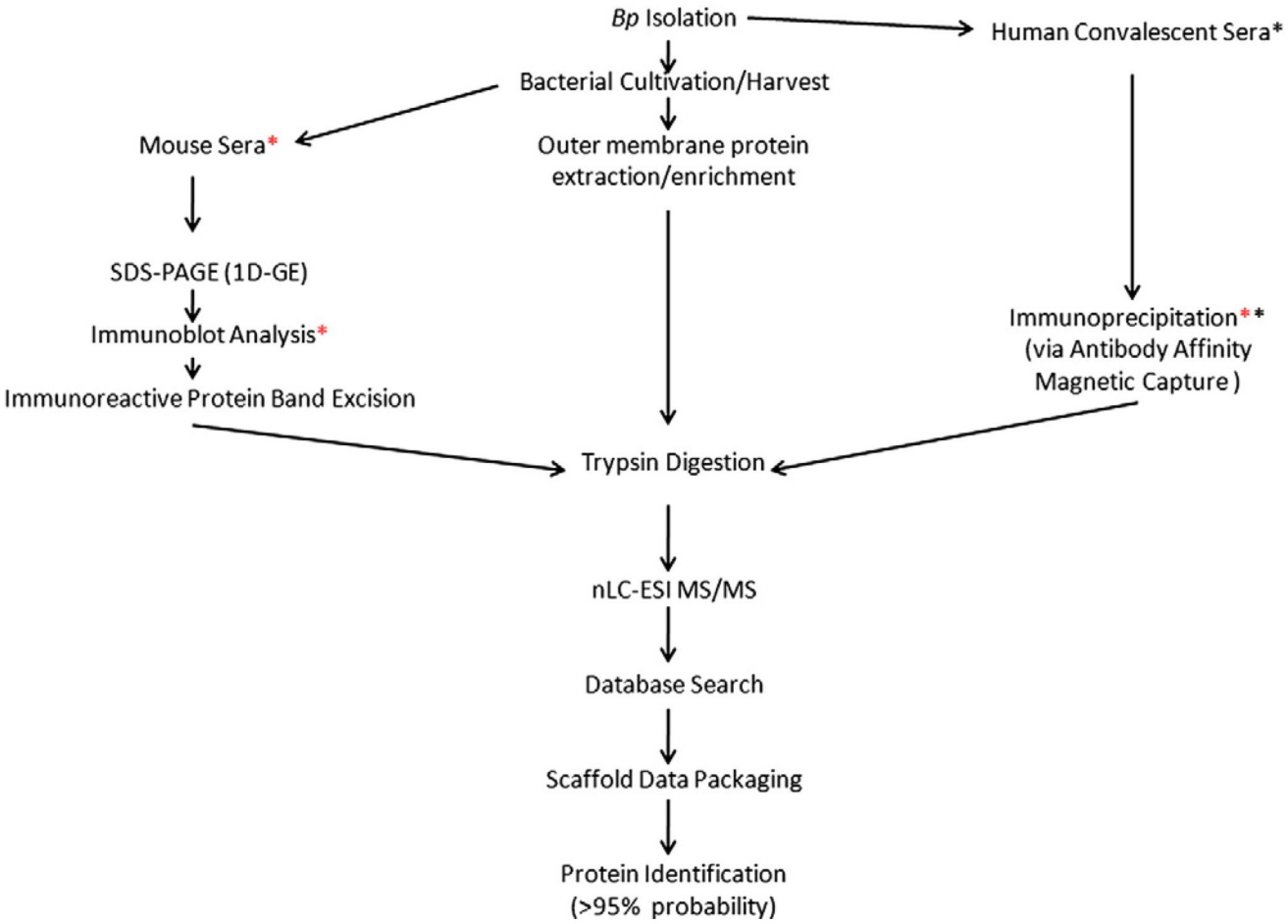

Fig. 1.

Flow diagram of core methodologies used in the proteomic study. Red Asterisk (*) indicates the mouse sera was used for the immunoblot analysis and immunoprecipitation. Black asterisk (*) indicates human convalescent sera was used for the immunoprecipitation.

Author Manuscript Author Manuscript Author Manuscript Author Manuscript

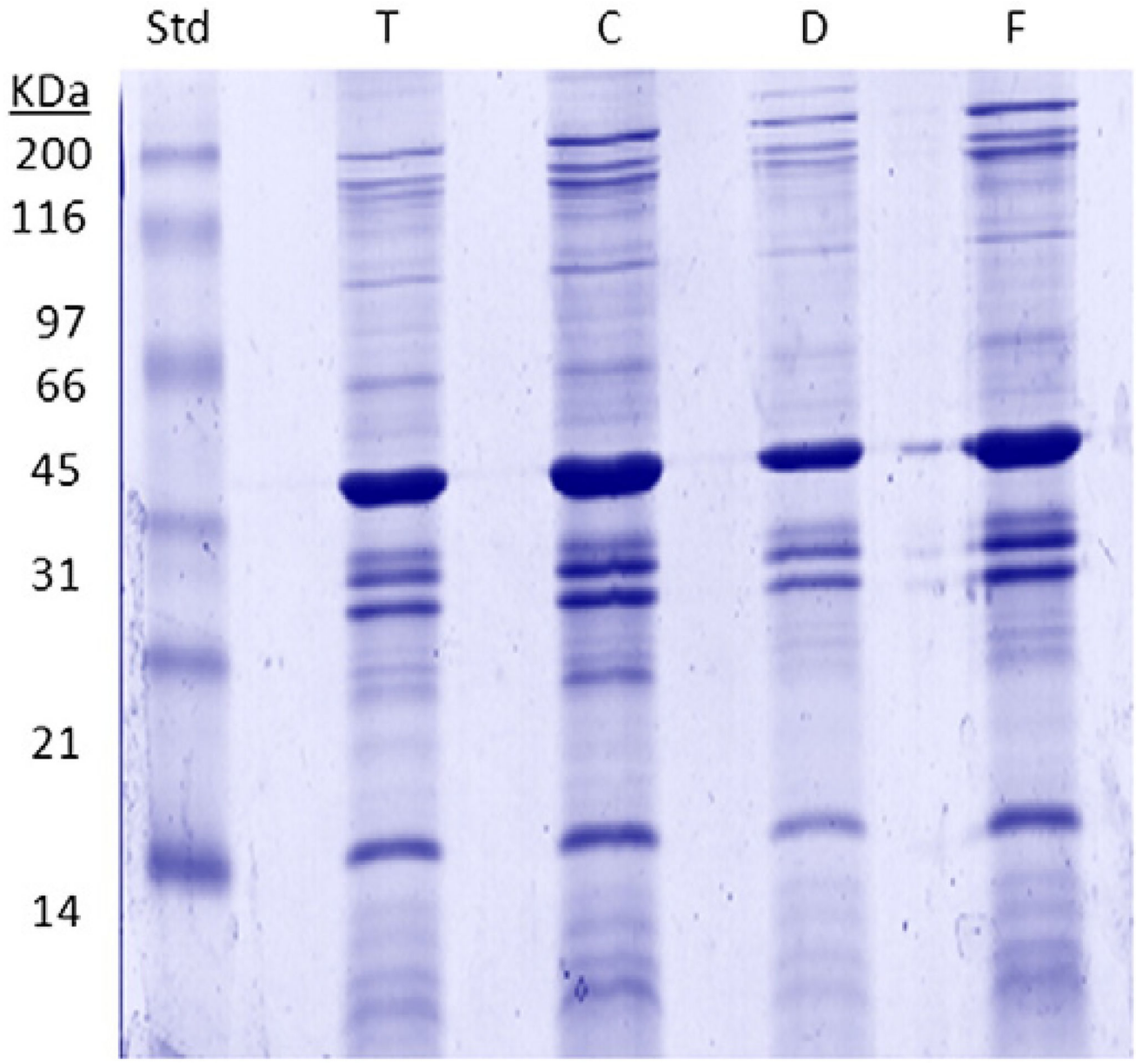

Fig. 2.

SDS-PAGE of *Bp* T, C, D, and F enriched membrane fractions (EMF). 10 μg of total carbonate-extracted EMF proteins from each strain was suspended in Laemmli sample buffer, electrophoresed on 12.5% SDS-PAGE gels, and stained using the hot coomassie blue staining protocol. Abbreviation: T — Tohama I, C — C056, D — D946 and F — F656; SDS-PAGE — sodium dodecyl sulfate-polyacrylamide gel electrophoresis.

Author Manuscript Author Manuscript Author Manuscript Author Manuscript

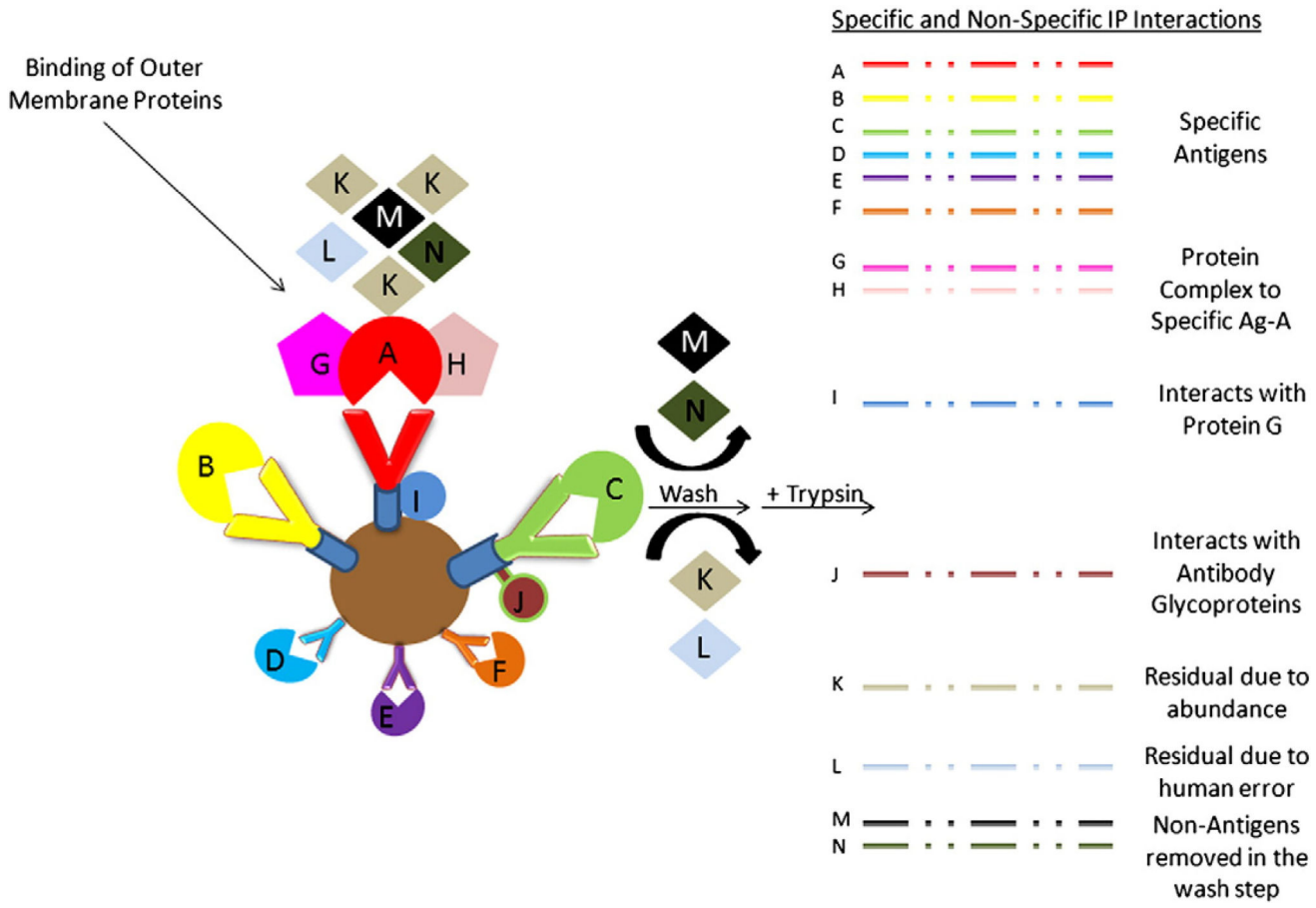

Fig. 3.

Illustration of potential specific and non-specific interactions during an immunoprecipitation (IP) from a biological and technical perspective.

Author Manuscript

Author Manuscript

Author Manuscript

Author Manuscript

Table 1

Genomic profiles of *Bordetella pertussis* (*Bp*) strains assessed in the study.

Strain	Isolation location (Year)	PFGE	Pertactin	Pertussis toxin
T	Japan (1954)	Type II	*prnA1*	*ptxS1B*
C	Minnesota, USA (1998)	CDC type I0	*prnA2*	*ptxS1A*
D	Georgia, USA (2002)	CDC type 21	*prnA1*	*ptxS1A*
F	Virgin Islands, USA (2007)	CDC type 206	*prnA2*	*ptxS1A*

Abbreviations: T — Tohama I, C — C056, D — D946 and F — F656; USA — United States of America; CDC — Centers for Disease Control and Prevention; PFGE — pulse field gel electrophoresis; Prn — pertactin; Ptx — pertussis toxin.

Author Manuscript Author Manuscript Author Manuscript Author Manuscript

Table 2

A Summary of the total number of *Bp* enriched membrane fraction (EMF) proteins commonly and uniquely identified among the *Bp* strains assessed in the study.

Strains	Total number of proteins
T	182
C	175
D	175
F	176
Strain combinations	**Total number of common proteins**
T, C, D, and F	163
T and C only	1
T and D only	3
T and F only	0
C and D only	0
C and F only	0
D and F only	0
T, C and D only	1
T, C and F only	5
T, D and F only	2
C, D and F only	3
Strains	**Total number of unique proteins**
T only	7
C only	2
D only	3
F only	3

Author Manuscript Author Manuscript Author Manuscript Author Manuscript

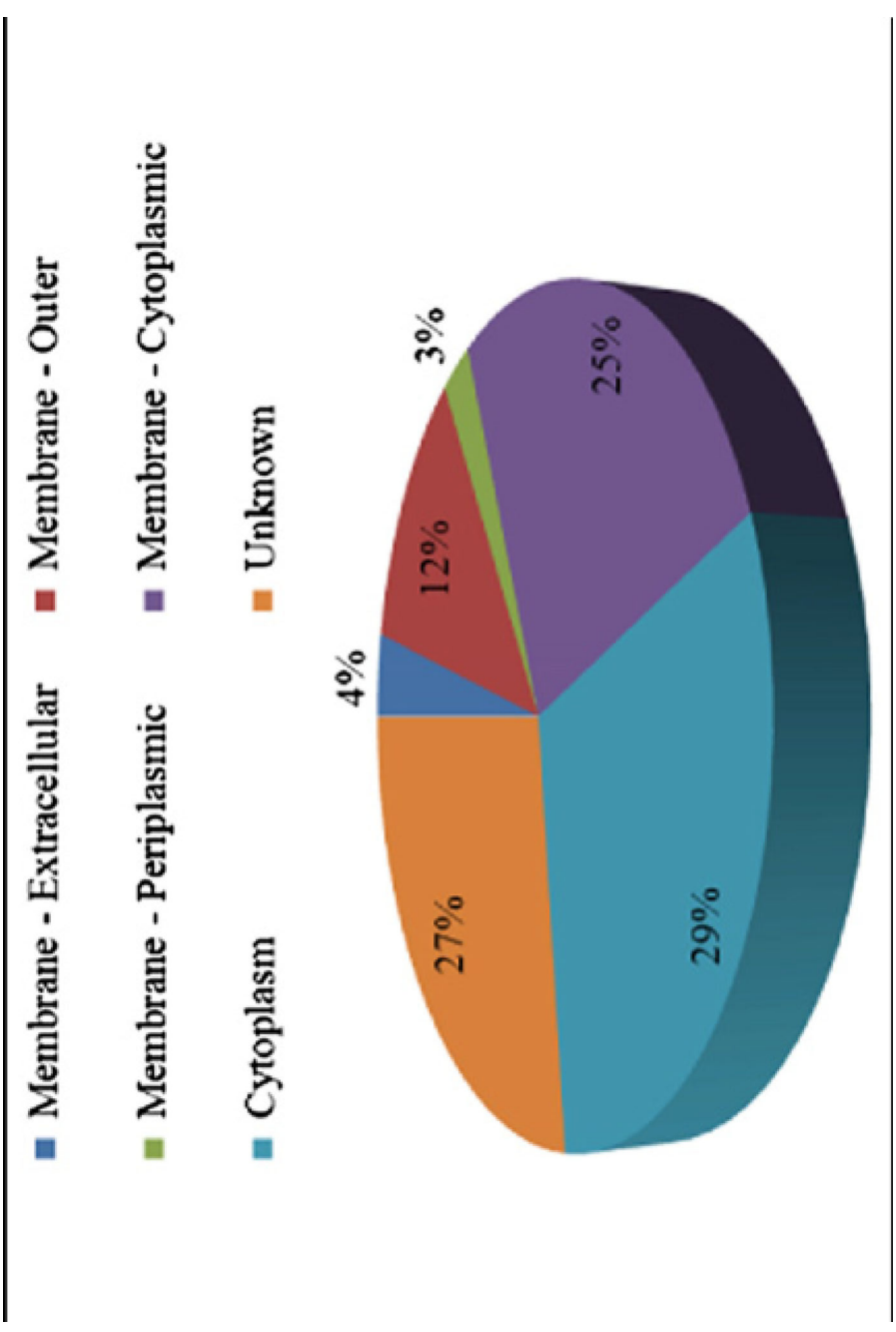

B Subcellular localization of identified *Bp* EMF proteins (— Table 2A).**

Author Manuscript Author Manuscript Author Manuscript Author Manuscript

C Protein function of identified *Bp* EMF proteins (— Table 2A).**

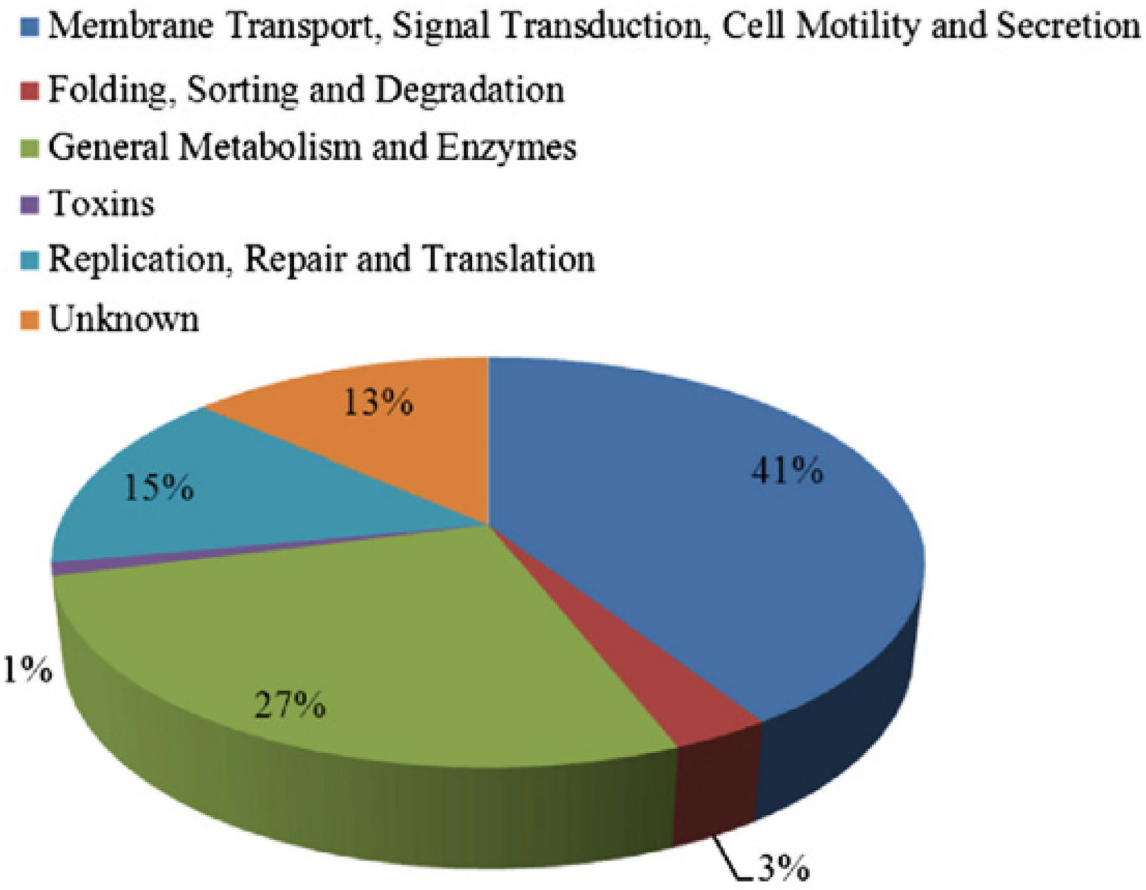

D Summary of *Bp* EMF proteins identified among *Bp* strains assessed in the study (— Table 2A).**

Protein	Accession #	ID	Gene	Size (kDa)	Location	T	C	D	F	Function
30S ribosomal protein S2	NP_880161	BP1419	rpsB	28	C	28 (4)	23 (3)	21 (3)	23 (3)	Translation
30S ribosomal protein S3	NP_882129	BP3619	rpsC	29	C	27 (4)	27 (4)	27 (5)	27 (4)	Translation
50S ribosomal protein L16	NP_882130	BP3620	rplP	15	C	26 (3)	36 (4)	19 (2)	29 (3)	Translation

Author Manuscript Author Manuscript Author Manuscript Author Manuscript

D Summary of *Bp* EMF proteins identified among *Bp* strains assessed in the study (— Table 2A).**

Protein	Accession #	ID	Gene	Size (kDa)	Location	T	C	D	F	Function
50S ribosomal protein L18	NP_882141	BP3632	rplR	13	C	20 (2)	20 (2)	30 (3)	20 (2)	Translation
50S ribosomal protein L2	NP_882126	BP3616	rplB	30	C	14 (3)	11 (2)	11 (2)	17 (3)	Translation
50S ribosomal protein L5	NP_882137	BP3628	rplE	20	C	17 (3)	12 (2)	12 (2)	18 (3)	Translation
50S ribosomal protein L6	NP_882140	BP3631	rplF	19	C	27 (3)	27 (3)	27 (3)	19 (2)	Translation
2-Isopropylmalate synthase	NP_879030	BP0131	leuA	62	U	6 (2)	14 (5)	8 (3)	11 (4)	Metabolism
5-Meta^	NP_881170	BP2543	metA	84	U	1 (1)	4 (2)	4 (2)	4 (2)	Metabolism
ABC transporter	NP_879529	BP0697	U	29	CM	22 (3)	22 (3)	27 (4)	28 (4)	Membrane transport
Acteyl-CoA carboxylase carboxyltransferase subunit alpha	NP_880596	BP1910	accA	35	C	17 (4)	29 (6)	24 (5)	17 (4)	Metabolism
Aconitate hydratase	NP_880684	BP2014	acnA	99	C	5 (3)	5 (3)	3 (2)	4 (2)	Metabolism
Acriflavine resistance protein B	NP_879779	BP0985	acrB	116	CM	6 (4)	3 (2)	5 (3)	3 (2)	Drug resistance
Adenylosuccinate lyase	NP_881474	BP2890	purB	50	C	7 (3)	5 (2)	9 (3)	9 (3)	Metabolism
Alanyl-tRNA synthetase	NP_880538	BP1836	alaS	96	C	15 (10)	9 (6)	8 (6)	8 (5)	Translation
ATP-dependent protease La	NP_880488	BP1777	Ion	90	C	5 (4)	5 (3)	6 (4)	5 (3)	Metabolism
Autotransporter	NP_880953	BP2315	vag8	101	OM/E	24 (15)	37 (22)	28 (18)	38 (22)	Transport
Autotransporter subtilisin-like protease	CAC44081	U	sphB1	114	OM/E	14 (9)	16 (9)	23 (15)	17 (10)	Transport
Bifunctional aconitate hydratase 2/2-methylisocitrate dehydratase	NP_880691	BP2021	acnB	95	C	8 (5)	6 (3)	9 (6)	6 (3)	Metabolism
Bifunctional hemolysin-adenylate cyclase precursor	NP_879578	BP0760	cyaA	188	E	8 (8)	18 (20)	10 (12)	14 (15)	Metabolism
Capsular polysaccharide biosynthesis protein	NP_880357	BP1629	wbpO	47	C	13 (3)	13 (3)	10 (2)	10 (2)	Metabolism
Cell division protein	NP_879861	BP1077	ftsH	69	CM	20 (9)	15 (6)	12 (6)	15 (7)	Cell division
Cell division protein FtsA	NP_881594	BP3019	ftsA	45	C	18 (5)	18 (5)	17 (5)	14 (4)	Cell division
Chain A, structure of the membrane protein Fhac	2QDZ_A	U	U	61	OM	22 (6)	26 (8)	25 (8)	27 (9)	Transport
Chaperonin GroEL	NP_882014	BP3495	groEL	60	C	16 (5)	13 (5)	20 (8)	12 (5)	RNA degradation
Competence lipoprotein	NP_879922	BP1146	comL	29	OM	21 (4)	12 (2)	26 (5)	16 (3)	Transport
Cytochrome C1 precursor	NP_879155	BP0275	petC	31	U	34 (6)	24 (4)	13 (3)	29 (4)	Metabolism
D-fructose-6-phosphate amidotransferase^	NP_879503	BP0666	glmS	67	C	7 (3)	4 (1)	10 (4)	8 (3)	Metabolism
Dihydrolipoamide acetyltransferase^	NP_879904	BP1125	odhB	44	CM	3 (1)	24 (4)	19 (3)	11 (2)	Metabolism
Dihydroorotate dehydrogenase 2	NP_881968	BP3442	pyrD	38	CM	21 (4)	18 (3)	18 (3)	13 (2)	Metabolism
Dihydroxy-acid dehydratase	NP_879169	BP0289	ilvD	68	C	7 (3)	5 (2)	5 (2)	5 (2)	Metabolism
DNA gyrase subunit B	NP_879342	BP0489	gyrB	90	C	4 (2)	7 (4)	3 (2)	5 (3)	DNA synthesis
DNA topoisomerase III^	NP_879317	BP0460	topB	96	C	9 (5)	9 (5)	8 (4)	2 (1)	DNA synthesis

Author Manuscript Author Manuscript Author Manuscript Author Manuscript

D Summary of *Bp* EMF proteins identified among *Bp* strains assessed in the study (— Table 2A).**

Protein	Accession #	ID	Gene	Size (kDa)	Location	T	C	D	F	Function
DNA-directed RNA polymerase subunit beta	NP_878932	BP0015	rpoB	151	C	3 (2)	7 (7)	5 (5)	4 (4)	Metabolism
DNA-directed RNA polymerase subunit beta	NP_878933	BP0016	rpoC	155	C	3 (3)	4 (4)	3 (4)	2 (2)	Metabolism
Elongation factor G	NP_882120	BP3610	fusA	77	C	26 (11)	24 (10)	13 (6)	20 (9)	Translation
Elongation factor Tu	NP_878925	BP0007	tuf	44	C	38 (9)	31 (7)	21 (5)	33 (8)	Translation
Enoyl- (acyl carrier protein) reductase^	NP_881766	BP3215	fabL	29	CM	5 (1)	9 (2)	9 (2)	4 (1)	Lipid metabolism
F0F1 ATP synthase subunit alpha^	NP_881828	BP3286	atpA	56	C	8 (3)	5 (2)	11 (4)	2 (1)	Energy metabolism
F0F1 ATP synthase subunit B	NP_881826	BP3284	atpF	17	CM	30 (4)	30 (4)	43 (6)	37 (5)	Energy metabolism
F0F1 ATP synthase subunit beta	NP_881830	BP3288	atpD	51	CM	17 (5)	23 (6)	7 (2)	15 (3)	Energy metabolism
Filamentous hemagglutinin/adhesion	NP_880571	BP1879	fhaB	394	OM	18 (43)	16 (37)	16 (38)	15 (34)	Adherence
Glutamate synthase [NADPH] large chain precursor	NP_882256	BP3753	qltb	174	C	7 (7)	3 (4)	2 (2)	6 (6)	Amino acid metabolism
Guanosine-3',5'-bis (diphosphate) 3'-pyrophosphohydrolase	NP_880309	BP1576	spoT	83	U	5 (3)	7 (4)	5 (3)	10 (6)	Nucleotide metabolism
Histone protein	NP_881561	BP2985	bpH1	19	C	18 (2)	18 (2)	18 (2)	18 (2)	DNA synthesis
HlyD family secretion protein^	NP_882313	BP3815	hlyD	46	CM	10 (2)	5 (1)	13 (3)	10 (2)	Signal transduction
Homoserine dehydrogenase^	NP_881384	BP2784	U	48	C	15 (4)	18 (5)	5 (1)	18 (5)	Amino acid metabolism
Hypothetical protein BP0162	NP_879055	BP0162	HP	37	U	14 (3)	9 (2)	23 (4)	23 (4)	HP
Hypothetical protein BP0205	NP_879093	BP0205	HP	21	U	44 (7)	47 (8)	39 (6)	44 (7)	HP/transport
Hypothetical protein BP0325^	NP_879200	BP0325	HP	43	CM	3 (1)	8 (3)	3 (1)	5 (2)	HP/membrane transport
Hypothetical protein BP0387	NP_879258	BP0387	HP	27	P	27 (4)	21 (3)	32 (5)	30 (4)	HP
Hypothetical protein BP0606	NP_879449	BP0606	HP	15	U	23 (2)	31 (3)	31 (3)	23 (2)	HP
Hypothetical protein BP1057	NP_879842	BP1057	HP	12	U	51 (3)	23 (2)	23 (2)	39 (2)	HP
Hypothetical protein BP1426	NP_880168	BP1426	HP	49	CM	20 (5)	11 (3)	7 (2)	11 (3)	HP
Hypothetical protein BP1438	NP_880180	BP1438	HP	16	U	16 (2)	16 (2)	15 (2)	16 (2)	HP
Hypothetical protein BP1440	NP_880182	BP1440	HP	34	U	42 (8)	36 (7)	44 (8)	42 (9)	HP/protein stability
Hypothetical protein BP1485	NP_880222	BP1485	HP	58	C	42 (12)	25 (8)	31 (9)	31 (D)	HP/protein transport
Hypothetical protein BP1903	NP_880589	BP1903	HP	58	CM	5 (2)	7 (2)	7 (3)	7 (2)	HP
Hypothetical protein BP2141^	NP_880795	BP2141	HP	17	U	9 (1)	24 (2)	24 (2)	31 (3)	HP
Hypothetical protein BP2191	NP_880839	BP2191	hflK	48	U	35 (8)	22 (5)	32 (8)	35 (9)	HP
Hypothetical protein BP2197	NP_880845	BP2197	HP	23	U	25 (3)	47 (6)	32 (4)	35 (4)	HP
Hypothetical protein BP2323	NP_880961	BP2323	HP	28	U	24 (3)	18 (2)	18 (2)	18 (2)	HP

Author Manuscript Author Manuscript Author Manuscript Author Manuscript

D Summary of *Bp* EMF proteins identified among *Bp* strains assessed in the study (— Table 2A).**

Protein	Accession #	ID	Gene	Size (kDa)	Location	T	C	D	F	Function
Hypothetical protein BP2534	NP_881161	BP2534	HP	58	U	25 (8)	18 (6)	18 (6)	17 (7)	HP/metabolism
Hypothetical protein BP2535	NP_881162	BP2535	HP	43	CM	34 (8)	34 (8)	14 (4)	29 (7)	HP/metabolism
Hypothetical protein BP2661^	NP_881275	BP2661	HP	32	U	10 (2)	5 (1)	10 (2)	10 (2)	HP/transport
Hypothetical protein BP2717	NP_881325	BP2717	HP	40	M/U	29 (5)	14 (3)	5 (2)	28 (5)	HP
Hypothetical protein BP2936	NP_881518	BP2936	HP	37	U	23 (6)	17 (4)	36 (9)	33 (8)	HP
Hypothetical protein BP3467	NP_881990	BP3467	HP	92	U	15 (7)	15 (7)	10 (5)	14 (7)	HP/membrane biogenesis
Hypothetical protein BP3521	NP_882036	BP3651	HP	61	C	7 (3)	6 (2)	5 (2)	7 (3)	HP/membrane biogenesis
Hypothetical protein BP3559	NP_882072	BP3559	HP	39	M/U	30 (6)	32 (6)	29 (6)	20 (4)	HP/cell division
Hypothetical protein BP3651	NP_882159	BP3651	HP	77	U	7 (3)	7 (3)	9 (4)	8 (3)	HP/membrane biogenesis
Hypothetical protein BP3689 (LysM domain/BON SFP)	NP_882194	BP3689	HP	20	U	24 (3)	22 (3)	22 (3)	22 (3)	HP/cell wall degradation
Hypothetical protein BP3758^	NP_882261	BP3758	HP	29	CM	3 (1)	5 (1)	7 (2)	7 (2)	HP/membrane transport
Hypothetical protein BP3819	NP_882317	BP3819	HP	27	U	12 (2)	23 (3)	19 (2)	19 (2)	HP
L-lactate dehydrogenase	NP_879338	BP0484	ildD	43	C	16 (4)	19 (3)	8 (2)	28 (6)	Carbohydrate metabolism
Large-conductance mechanosensitive channel	NP_879158	BP0278	mscl	17	U	25 (3)	25 (3)	13 (2)	25 (3)	Transport
Lipoprotein^	NP_881354	BP2750	HP	24	U	13 (2)	13 (2)	11 (2)	7 (1)	U
Lipoprotein	NP_879963	BP1189	U	16	U	24 (2)	39 (3)	39 (3)	25 (2)	U
Mce related protein	NP_882262	BP3759	U	18	U	59 (4)	35 (2)	73 (5)	45 (3)	Transport
Outer membrane lipoprotein	NP_881135	BP2508	omlA	20	OM	34 (3)	29 (3)	40 (4)	47 (5)	Transport
Outer membrane porin protein OmpQ	NP_881933	BP3405	ompQ	40	OM	30 (8)	27 (7)	23 (6)	29 (8)	Transport
Outer membrane porin protein precursor	NP_879650	BP0840	U	42	OM	52 (12)	43 (10)	47 (10)	43 (10)	Transport
Outer membrane protein A precursor	NP_879744	BP0943	ompA	21	OM	44 (7)	39 (5)	39 (6)	44 (6)	Transport
Outer membrane usher protein precursor	NP_880573	BP1882	fimC	96	OM	10 (6)	11 (6)	13 (9)	11 (7)	Membrane biogenesis
Penicillin-binding protein 1A	NP_882163	BP3655	U	90	E	9 (3)	11 (4)	10 (4)	11 (5)	Peptidoglycan metabolism
Putative peptidoglycan-associated lipoprotein	NP_881875	BP3342	U	18	OM	59 (7)	59 (6)	67 (8)	53 (7)	Transport
Peptidyl-prolyl cis-trans isomerase D	NP_880447	BP1732	ppiD	7	U	45 (16)	38 (13)	38 (14)	36 (12)	Protein folding
Pertactin	BAF35031	U	prn	101	OM	21 (13)	17 (11)	14 (8)	15 (9)	Transport
Phosphoenolpyruvate synthase	NP_880178	BP1436	ppsA	87	C	9 (6)	3 (2)	5 (3)	3 (2)	Carbohydrate metabolism
Phosphoglucomutase/phosphomannomutase	NP_879859	BP1075	qlmM	50	C	9 (3)	6 (2)	6 (2)	6 (2)	Carbohydrate metabolism
Preprotein translocase subunit SecA	NP_881589	BP3014	secA	100	CM	10 (7)	6 (4)	2 (2)	2 (2)	Membrane transport
Preprotein translocase subunit SecD	NP_879831	BP1046	secD	69	CM	28 (11)	23 (10)	29 (11)	26 (10)	Membrane transport

Author Manuscript Author Manuscript Author Manuscript Author Manuscript

D Summary of *Bp* EMF proteins identified among *Bp* strains assessed in the study (— Table 2A).**

Protein	Accession #	ID	Gene	Size (kDa)	Location	T	C	D	F	Function
Preprotein translocase subunit SecF	NP_879830	BP1045	secF	34	CM	19 (3)	19 (3)	19 (3)	19 (3)	Membrane transport
Preprotein translocase subunit SecG	NP_879617	BP0802	secG	16	U	41 (2)	41 (2)	41 (2)	41 (2)	Membrane transport
Putative ABC transporter	NP_880959	BP2321	Pu	69	CM	16 (5)	10 (3)	15 (4)	15 (4)	Transport
Putative ABC transporter ATP-binding subunit^	NP_881029	BP2397	Pu	70	CM	7 (2)	8 (2)	2 (1)	5 (1)	Membrane transport
Putative ABC transporter ATP-binding subunit^	NP_880660	BP1986	Pu	70	CM	3 (1)	11 (4)	7 (2)	7 (2)	Membrane transport
Putative ABC transporter ATP-binding subunit	NP_882260	BP3757	Pu	31	CM	19 (3)	29 (4)	29 (4)	23 (4)	Membrane transport
Putative ABC transporter ATP-binding subunit	NP_880723	BP2057	Pu	46	CM	34 (7)	28 (6)	6 (2)	24 (5)	Membrane transport
Putative amino acid ABC transporter ATP-binding protein	NP_882326	BP3828	Pu	27	CM	20 (3)	15 (2)	20 (3)	15 (2)	Membrane transport
Putative amino acid ABC transporter permease protein	NP_882328	BP3830	Pu	44	CM	13 (3)	8 (2)	8 (2)	8 (2)	Membrane transport
Putative bifunctional protein	NP_882247	BP3744	Pu	43	CM	22 (6)	17 (4)	12 (3)	17 (4)	Energy metabolism
Putative binding-protein-dependent transport permease	NP_881026	BP2394	Pu	33	CM	5 (1)	3 (1)	7 (2)	5 (1)	Membrane transport
Putative binding-protein-dependent transport protein	NP_881859	BP3322	Pu	42	P	41 (7)	27 (6)	33 (6)	26 (4)	Membrane transport
Putative cell division protein^	NP_881100	BP2473	Pu	87	CM	5 (2)	2 (1)	4 (1)	4 (3)	Cell division
Putative chromosome partition protein	NP_882071	BP3558	Pu	130	C	7 (6)	11 (7)	9 (6)	8 (6)	Cell division
Putative dioxygenase	NP_880971	BP2333	Pu	34	CM	16 (3)	19 (4)	11 (2)	19 (4)	Amino acid metabolism
Putative efflux system inner membrane protein	NP_880738	BP2075	Pu	49	CM	14 (4)	18 (5)	14 (4)	14 (4)	Membrane transport
Putative efflux system transmembrane protein	NP_880739	BP2076	Pu	118	CM	12 (9)	5 (4)	8 (7)	10 (7)	Membrane transport
Putative exported solute binding protein	NP_881542	BP2963	Pu	40	U	17 (4)	10 (2)	10 (2)	13 (3)	Membrane transport
Putative extracellular solute-binding protein	NP_880657	BP1983	Pu	82	P	6 (3)	6 (3)	6 (3)	6 (3)	Membrane transport
Putative glycosyl transferase	NP_881785	BP3238	Pu	34	U	20 (4)	10 (2)	12 (2)	22 (4)	Metabolism
Putative inner membrane protein	NP_881862	BP3326	Pu	26	U	27 (4)	27 (4)	28 (4)	49 (6)	HP
Putative inner membrane protein translocase component YidC	NP_886531	BBP4405	Pu	62	CM	9 (3)	15 (4)	12 (4)	7 (3)	Membrane transport
Putative inner membrane-anchored protein	NP_880838	BP2190	Pu	33	U	16 (4)	20 (5)	20 (4)	15 (3)	HP
Putative integral membrane protein	NP_881049	BP2420	Pu	41	CM	9 (2)	12 (2)	16 (4)	7 (2)	Membrane transport
Putative L-lactate dehydrogenase	NP_879251	BP0379	Pu	39	C	7 (2)	18 (3)	18 (3)	21 (4)	Carbohydrate metabolism
Putative lipoprotein	NP_880735	BP2072	Pu	22	U	24 (3)	27 (3)	24 (3)	18 (2)	Putative transport
Putative lipoprotein	NP_881568	BP2992	Pu	18	OM	59 (6)	49 (5)	53 (5)	53 (5)	Putative transport
Putative lipoprotein	NP_882263	BP3760	Pu	29	OM	13 (2)	25 (4)	16 (4)	11 (3)	Putative transport
Putative lipoprotein	NP_880063	BP1296	Pu	30	U	16 (3)	12 (2)	12 (2)	12 (2)	U
Putative lipoprotein	NP_880303	BP1296	Pu	41	U	26 (5)	30 (6)	22 (5)	30 (7)	Putative membrane

Author Manuscript Author Manuscript Author Manuscript Author Manuscript

D Summary of *Bp* EMF proteins identified among *Bp* strains assessed in the study (— Table 2A).**

Protein	Accession #	ID	Gene	Size (kDa)	Location	T	C	D	F	Function
Putative lipoprotein	NP_880710	BP2043	Pu	24	U	26 (4)	15 (2)	23 (4)	11 (2)	U
Putative membrane transport ATPase	NP_881330	BP2722	Pu	86	CM	4 (2)	4 (2)	3 (2)	5 (2)	Putative transport
Putative membrane transport protein	NP_881309	BP2716	Pu	49	U	7 (2)	7 (2)	11 (3)	7 (2)	Putative transport
Putative NADH dehydrogenase	NP_882010	BP3491	ndh	48	CM	10 (3)	6 (2)	6 (2)	6 (2)	Energy metabolism
Putative outer membrane (permeability) protein	NP_881865	BP3329	Pu	87	OM	16 (7)	9 (4)	12 (6)	10 (5)	Putative transport
Putative outer membrane ligand binding protein	NP_879893	BP1112	bipA	144	OM	39 (28)	15 (12)	23 (17)	13 (12)	Adherence
Putative peptidase	NP_880436	BP1721	Pu	32	OM	22 (3)	20 (3)	20 (3)	27 (4)	Protein degradation
Putative quinoprotein	NP_880844	BP2196	Pu	42	OM	31 (6)	29 (5)	38 (7)	20 (4)	Protein assembly
Putative secreted protein^	NP_879832	BP1047	Pu	13	U	32 (2)	32 (2)	32 (2)	21 (1)	Membrane transport
Putative secretion system protein	NP_882292	BP3793	ptle	26	U	14 (3)	21 (4)	17 (3)	16 (3)	Putative transport
Putative secretion system protein	NP_882293	BP3794	ptlf	30	U	11 (2)	19 (3)	19 (3)	11 (2)	Putative transport
Putative secretion system protein	NP_882289	BP3794	ptlc	91	CM	6 (3)	9 (5)	9 (5)	11 (6)	Putative transport
Putative sugar transport protein^	NP_881176	BP2549	Pu	61	CM	5 (2)	2 (1)	5 (2)	5 (2)	Putative transport
Putative sulfatase	NP_881701	BP3136	Pu	72	CM	21 (8)	10 (5)	17 (8)	17 (8)	Membrane biogenesis
Putative TolQ-like translocation protein	NP_881879	BP3346	Pu	25	CM	22 (3)	22 (3)	23 (4)	19 (3)	Membrane transport
Putative type III secretion protein	NP_880879	BP2235	Pu	66	CM	8 (3)	10 (3)	12 (5)	12 (4)	Membrane transport
Pyrroline-5-carboxylate reductase	NP_880048	BP1280	proC	30	C	15 (3)	15 (3)	10 (2)	11 (2)	amino acid metabolism
RecA	AAK85426	U	recA	31	C	36 (6)	31 (5)	28 (4)	22 (4)	DNA processing
Ribonuclease E	NP_879331	BP0475	rne	115	C	12 (8)	8 (5)	6 (4)	8 (5)	RNA degradation
Ribonucleotide-diphosphate reductase subunit alpha	NP_881559	BP2983	nrdA	107	C	10 (7)	5 (3)	3 (2)	8 (5)	Nucleotide metabolism
RNA polymerase sigma 80 subunit	AAC45085	BP1191	rpoD	81	C	9 (4)	5 (2)	6 (3)	6 (2)	RNA processing
Rod shape-determining protein	NP_879246	BP0374	mreB	38	C	16 (3)	19 (4)	8 (2)	12 (3)	Cell morphology
SCO1/SenC family protein^	NP_882237	BP3734	U	22	U	17 (3)	6 (1)	10 (2)	6 (1)	Transport
Serum resistance protein	NP_882013	BP3494	brkA	111	OM	23 (14)	27 (14)	29 (17)	38 (21)	Transport
Signal peptidase I	NP_881060	BP2432	lep	32	CM	11 (2)	19 (4)	14 (3)	12 (2)	Transport
Succinate dehydrogenase flavoprotein subunit^	NP_880997	BP2361	sdhA	65	CM	7 (3)	7 (3)	3 (1)	11 (5)	Carbohydrate metabolism
Succinate dehydrogenase iron–sulfur protein^	YP_785707	BAV1185	sdhB	26	CM	4 (1)	14 (4)	9 (3)	14 (3)	Carbohydrate metabolism
Succinyl-CoA synthetase subunit beta	NP_881168	BP2541	sucC	42	U	14 (3)	9 (2)	9 (2)	17 (4)	Carbohydrate metabolism
Surface antigen	NP_880169	BP1427	U	86	OM	29 (15)	29 (15)	25 (13)	35 (18)	Protein assembly

J Microbiol Methods. Author manuscript; available in PMC 2017 November 15.

Author Manuscript Author Manuscript Author Manuscript Author Manuscript

D Summary of *Bp* EMF proteins identified among *Bp* strains assessed in the study (— Table 2A).**

Protein	Accession #	ID	Gene	Size (kDa)	Location	T	C	D	F	Function
Tex	CAA64672	BP1144	tex	87	C	5 (3)	4 (2)	3 (2)	4 (2)	RNA processing
Thiol:disulfide interchange protein	NP_882154	BP3646	DsbA	71	CM	15 (7)	14 (6)	14 (6)	10 (4)	Membrane biogenesis
Threonine synthase	NP_881383	BP2783	thrC	51	C	16 (5)	31 (9)	10 (3)	17 (5)	Amino acid metabolism
TonB-dependent receptor for iron transport	NP_879666	BP0856	bfrD	82	OM	34 (20)	35 (21)	29 (18)	28 (15)	Membrane transport
Tracheal colonization factor precursor	NP_879974	BP1201	tcfA	71	OM	12 (6)	20 (8)	19 (10)	10 (6)	Membrane transport
Translocation protein TolB	NP_881876	BP3343	tolB	48	P	13 (3)	15 (4)	21 (6)	14 (4)	Transport
Trifunctional transcriptional regulator/proline DH/P-5-C DH	NP_881353	BP2749	putA	140	C	11 (9)	10 (8)	14 (12)	14 (12)	Amino acid metabolism
Twin argininte translocase protein A	NP_882278	BP3777	tatA	8	U	35 (2)	35 (2)	35 (2)	35 (2)	Membrane transport
Type II citrate synthase	NP_880994	BP2358	qltA	48	C	11 (3)	8 (2)	10 (3)	10 (3)	Carbohydrate metabolism
Ubiquinol oxidase polypeptide I	NP_881514	BP2932	cyoB	72	CM	6 (3)	6 (2)	9 (4)	6 (2)	Energy metabolism
Uridylate kinase	NP_880163	BP1421	pyrH	26	C	13 (3)	10 (2)	23 (4)	16 (3)	Nucleotide metabolism
Virulence factors transcription regulator	NP_880570	BP1878	bvgA	23	C	43 (7)	59 (9)	52 (8)	34 (5)	Signal transduction
DNA polymerase I	NP_880026	BP1254	polA	99	C	5 (3)	5 (3)			Nucleotide metabolism
Acetyl-CoA synthetase	NP_881040	BP2409	acsA	72	C	6 (3)		4 (2)		Carbohydrate metabolism
2-Oxoglutarate dehydrogenase E1 component[^]	NP_879903	BP1124	sucA	106	C	2 (1)		4 (2)		Metabolism
Probable Orn/Arg/Lys decarboxylase[^]	NP_879079	BP0190	U	83	C	3 (1)		4 (2)		Amino acid metabolism
Autotransporter	NP_879378	BP0529	U	246	OM/E	7 (2)	5 (6)		2 (2)	Membrane transport
Cytochrome B[^]	NP_879156	BP0276	petB	51	CM	17 (5)	3 (1)		5 (2)	Energy metabolism
DNA mismatch repair protein[^]	NP_879129	BP0244	mutL	69	C	4 (2)	6 (2)		5 (1)	DNA processing
HP BP3084	NP_881655	BP3084	HP	41	C	18 (4)	17 (4)		10 (2)	HP
Ubiquinol-cytochrome C reductase iron–sulfur subunit	NP_879157	BP0277	petA	23	CM	24 (3)	24 (3)		19 (2)	Energy metabolism
30s ribosomal protein S20[^]	NP_881377	BP2773	rspT	90	U	14 (2)	13 (1)	14 (2)		Translation
Putative membrane-bound transglycosylase[^]	NP_881812	BP3268	Pu	47	OM	4 (1)		14 (4)	16 (4)	Membrane biogenesis
Putative transglycosylase[^]	NP_881631	BP3060	Pu	76	P	4 (2)		4 (1)	4 (1)	Membrane biogenesis
Dermonecrotic toxin	NP_881965	BP3439	dnt	161	U		5 (4)	2 (2)	4 (4)	Cell death
Putative periplasmic solute-binding	NP_880224	BP1487	smoM	40	U		8 (2)	8 (2)	16 (4)	Putative transport
Serotype 3 fimbrial subunit	NP_880302	BP1568	fim3	22	E		20 (3)	27 (4)	15 (2)	Cell integrity
CTP synthetase (synthase)	NP_881022	BP2389	pyrG	61	C	5 (2)				Nucleotide metabolism
Cycolysin secretion protein	NP_879580	BP0762	cyaD	48	CM	12 (3)				Membrane transport

Author Manuscript Author Manuscript Author Manuscript Author Manuscript

D Summary of *Bp* EMF proteins identified among *Bp* strains assessed in the study (— Table 2A).**

Protein	Accession #	ID	Gene	Size (kDa)	Location	T	C	D	F	Function
HP BP1123	NP_879902	BP1123	HP	75	U	11 (5)				HP
Putative ketopantoate reductase	NP_880110	BP1360	Pu	34	C	10 (2)				HP/metabolism
Putative transcriptional regulation protein	NP_881198	BP2571	Pu	15	U	27 (2)				HP/RNA processing
Serotype 2 fimbrial subunit	P05788	BP1119	fim2	23	E	21 (2)				Cell integrity
Threonyl-tRNA-synthetase	NP_880233	BP1497	thrS	71	C	8 (3)				Translation
ABC transport protein, ATP-binding component	NP_881414	BP2816	metN	40	CM		10 (2)			Membrane transport
HP BP3441	NP_881967	BP3441	HP	36	M/U		19 (3)			HP
BpH2 (novel histone — 18323)	AAB40156	U	bph2	16	U			19 (2)		DNA processing
Putative heme receptor	NP_879314	BP0456	hemC	82	OM			6 (3)		Membrane transport
Trigger factor	NP_880485	BP1774	tig	48	U			8 (2)		Cell division
Exopolyphosphatase	NP_879857	BP1073	ppx	55	C				4 (2)	Nucleotide metabolism
HP BP2486	NP_881113	BP2486	HP	45	CM				8 (2)	HP
HP BP3002	NP_881577	BP3002	HP	69	C				6 (2)	HP

Numerical values are based on a greater that 95% Scaffold protein identification probability**.

Abbreviations: T — Tohama I, C — C056, D — D946 and F — F656.

PSORTb subcellular scores were used to predict and localize the identified EMF proteins.

KEGG identifiers were employed to assign functions to each of the identified EMF proteins.

NCBI Gi accession numbers were used to further compile information such as gene identification number, subcellular localization (PSORTb) and protein function (KEGG identifiers). Values noted represent percent amino acid coverage of the identified EMF protein. (Number of unique peptides detected in parenthesis.).

(^) indicates that identified proteins only had one unique detected tryptic peptide. No numerical value noted indicates that the protein was not identified in the strain.

Abbreviations: T — Tohama I, C — C056, D — D946 and F — F656; OM — outer membrane, CM — cytoplasmic membrane, C — cytoplasm, P — periplasm, E — extracellular, M — membrane, U — unknown, Pu — putative, HP — hypothetical protein; DH (dehydrogenase), P-5-C-DH (pyrroline-5-carboxylate DH), SFP (superfamily protein), 5-meta (5-methyltetrahydropteroyltriglutamate–homocysteine methyltransferase); BBP — *B. parapertussis*, BB — *B. bronchiseptica*, BAV – *B. avium*.

Author Manuscript Author Manuscript Author Manuscript Author Manuscript

Table 3

A Summary of identified *Bp* putative immunogenic proteins using the mouse model (— Table 2A).**

	T	C	D	F
Total PIPs	19	31	31	12
Total PIPs with CR or NS with normal mouse IgG bound-beads	6	7	12	4
Total PIPS without CR or NS with normal IgG bound-beads	13	24	19	8
% of total surfaceome (EMF) with tentative antigenic protein potential	11%	18%	18%	7%

B Putative *Bp* immunogenic proteins identified among *Bp* strains assessed in the study.

Protein	Accession #	Size (KDa)	Localization	T	C	D	F
Autotransporter (Vag8)	NP_880953	101	OM/E		11(6)*	16(10)*	5(3)
Chaperonin GroEL	NP_882014	60	C		12(4)	14(5)	
Elongation factor Ts	CAE33099	34	C		19(5)		
Elongation factor Tu	NP_878925	44	C		8(2)	15(4)	
F0F1 ATP synthase subunit B^	NP_881826	17	CM			10(1)	
Fructose-1,6-bisphosphate aldolase	NP_880254	39	C		14(4)		
Glyceraldehyde-3-phosphate dehydrogenase	NP_879794	37	C		8(2)		
HP BB 4955	NP_891489	74	U	6(2)			
HP BP 0205	NP_879093	21	U	10(2)		22(2)*	
HP BP 0455	NP_879313	74	U	3(1)			
HP BP 1057	NP_879842	12	U			23(2)	
HP BP 1440^	NP_880182	34	U	22(4)*	12(2)*	34(6)*	8(1)
HP BP 1485^	NP_880222	58	C		3(1)*	15(6)*	
HP BP 2191	NP_880839	48	U	7(2)*		8(2)	
ketol-acid reductoisomerase	NP_879606	37	C		13(3)		
N-acetyl-gamma-glutamyl-phosphate reductase	NP_881539	39	C		16(4)		
Outer membrane porin protein OmpQ	NP_881933	40	OM	8(2)	8(2)*	13(3)*	8(2)

Author Manuscript Author Manuscript Author Manuscript Author Manuscript

B Putative *Bp* immunogenic proteins identified among *Bp* strains assessed in the study.

Protein	Accession #	Size (KDa)	Localization	T	C	D	F
Outer membrane porin protein precursor	NP_879650	42	OM	30(7)*	50(13)*	35(9)*	35(9)*
Outer membrane protein A precursor	NP_879744	21	OM	17(4)*	21(5)*	17(4)*	35(4)*
Pertactin^	BAF35031	101	OM	6(3)	4(2)	2(1)	
Phospho-2-dehydro-3-deoxyheptonate aldolase	NP_881490	39	C		13(3)		
Preprotein translocase subunit SecD	NP_879831	69	CM		5(2)	7(3)*	5(2)
Putative bifunctional protein	NP_882247	43	CM			8(2)	
Putative binding-protein-dependent^	NP_881859	42	P	10(2)	12(3)	3(1)	
Putative efflux system transmembrane…^	NP_880739	118	CM	4(2)	2(1)		
Putative exported solute binding protein	NP_881542	40	U		8(2)		
Putative inner membrane protein	NP_881862	26	U	15(2)			
Putative inner membrane protein	NP_886531	62	CM			6(2)	
Putative inner membrane-anchored protein	NP_880838	33	U	8(2)		8(2)	
Putative L-lactate dehydrogenase	NP_879251	39	C		11(3)		
Putative lipoprotein	NP_881568	18	OM	44(4)	14(2)	49(5)*	35(3)*
Putative lipoprotein	NP_880303	41	U		12(3)		
Putative outer membrane ligand binding protein	NP_879893	144	OM	4(3)			
Putative peptidase	NP_880436	32	OM			16(2)	
Putative peptidoglycan-associated lipoprotein^	NP_881875	18	OM		17(2)	29(3)*	7(1)
Putative periplasmic solute-binding protein	NP_880224	40	U		15(4)		
Putative secreted protein^	NP_879832	13	U		21(1)	32(2)	
Putative sulfatase	NP_881701	72	CM			4(2)	
Probable inner-membrane protein	CAE35357	61	CM			6(2)	
Rod-shape determining protein	NP_879246	38	C		16(4)		
SCO1/SenC family protein^	NP_882237	22	U		6(1)	6(1)	6(1)

J Microbiol Methods. Author manuscript; available in PMC 2017 November 15.

Author Manuscript Author Manuscript Author Manuscript Author Manuscript

B Putative *Bp* immunogenic proteins identified among *Bp* strains assessed in the study.

Protein	Accession #	Size (KDa)	Localization	T	C	D	F
Serotype 3 fimbrial subunit	NP_880302	22	E			17(2)	
Serum resistance protein (BrkA)	NP_882013	111	OM	4(3)*	3(2)	4(3)	4(3)
Signal peptidase I	NP_881060	32	CM			7(2)	
Surface antigen	NP_880169	86	OM	6(3)			
Thiol:disulfide interchange protein	NP_882154	71	CM		3(2)	3(2)*	3(2)
TonB-dependent receptor for iron transport	NP_879666	82	OM	4(2)	5(3)	13(7)	
Tracheal colonization factor precursor	NP_879974	71	OM	6(3)*	7(3)*	7(3)*	9(4)*

Abbreviations: T — Tohama I, C — C056, D — D946 and F — F656; CR — cross-reactivity, NS — non-specificity, IgG — immunoglobulin G, EMF — enriched membrane fraction, PIPs — putative immunogenic proteins.

Values noted represent percent amino acid coverage of the identified IP protein using the mouse model. (Number of unique peptides detected in parenthesis.). No numerical value noted indicates that the protein was not identified in the mouse IP.

(^)indicates that identified proteins only had one unique detected tryptic peptide.

Asterisk (*) indicates that the protein identified in the mouse IP was cross-reactive with normal mouse IgG-bound beads. Blue-shaded box: common in all 3 clinical isolates; black-bordered box: common in all 4 strains.

Abbreviations: T — Tohama I, C — C056, D — D946 and F — F656; OM — outermembrane, CM — cytoplasmic membrane, C — cytoplasm, P — periplasm, E — extracellular, M — membrane, U — unknown, HP — hypothetical protein, BB — *B. bronchiseptica*.

Author Manuscript Author Manuscript Author Manuscript Author Manuscript

Table 4

A Summary of identified *Bp* putative immunogenic proteins using the human model (— Table 2A).**

	T	C	D	F
Total PIPs	4	12	8	10
Total PIPs with CR or NS with normal mouse IgG bound-beads	3	9	8	7
Total PIPS without CR or NS with normal IgG bound-beads	1	3	0	3
% of total surfaceome (EMF) with tentative antigenic protein potential	1%	2%	0%	2%

B Putative *Bp* immunogenic proteins identified among *Bp* strains assessed in the study.

Protein	Accession #	T	C	D	F
Autotransporter (Vag8)	NP_880953		12(8)*	17(12)*	7(4)*
HP BP 0205^	NP_879093		6(1)*		21(4)
HP BP 1440	NP_880182	10(3)		27(5)*	11(3)
HP BP 1485	NP_880222		9(3)*	16(7)*	6(2)
HP BP 3689	NP_882194				18(2)
Outer membrane porin protein OmpQ^	NP_881933	3(1)*	7(2)*	11(3)*	4(1)*
Outer membrane porin protein precursor	NP_879650	23(6)*	21(7)*		
Outer membrane protein A precursor	NP_879744	10(3)*	21(5)*	21(5)*	17(3)*
Preprotein translocase subunit SecD	NP_879831			12(5)*	
Probable inner membrane protein	CAE35357		4(2)*		
Putative lipoprotein	NP_881568		37(3)*		22(2)*
Serum resistance protein (BrkA)	NP_882013		2(2)*		
Thiol:disulfide interchange protein	NP_882154		3(2)		
TonB-dependent receptor for iron transport	NP_879666		7(4)	19(11)*	3(2)
Tracheal colonization factor protein	NP_879974		9(4)*	10(5)*	7(3)*

Abbreviations: T — Tohama I, C — C056, D — D946 and F — F656; CR — cross-reactivity; NS — non-specificity; IgG — immunoglobulin G; EMF — enriched membrane fraction; PIPs — putative immunogenic protein.

Author Manuscript Author Manuscript Author Manuscript Author Manuscript

Values noted represent percent amino acid coverage of the identified IP protein using the human model. (Number of unique peptides detected in parenthesis.). No numerical value noted indicates that the protein was not identified in the human IP.

(^) indicates that identified proteins only had one unique detected tryptic peptide.

Asterisk (*) indicates that the protein identified in the human IP was cross-reactive with normal human IgG-bound beads. Pink-shaded box — protein identified in human and mouse IP; yellow-shaded box — strain-specific protein identification only in human IP; black-bordered box: common in all 4 strains.

Abbreviation: T — Tohama I, C — C056, D — D946 and F — F656.